






ORIGINAL RESEARCH

# Impact of NKG2D Signaling on Natural Killer and T-Cell Function in Cerebral Ischemia

Christina David , MSc\*; Tobias Ruck , MD\*; Leoni Rolfes, MD; Stine Mencl, PhD; Peter Kraft, MD; Michael K. Schuhmann, PhD; Christina B. Schroeter, MD; Robin Jansen, MD; Friederike Langhauser , PhD; Anne K. Mausberg , PhD; Anke C. Fender, PhD; Sven G. Meuth, MD, PhD\*; Christoph Kleinschnitz , MD\*

**BACKGROUND:** Typically defined as a thromboinflammatory disease, ischemic stroke features early and delayed inflammatory responses, which determine the extent of ischemia-related brain damage. T and natural killer cells have been implicated in neuronal cytotoxicity and inflammation, but the precise mechanisms of immune cell-mediated stroke progression remain poorly understood. The activating immunoreceptor NKG2D is expressed on both natural killer and T cells and may be critically involved.

**METHODS AND RESULTS:** An anti-NKG2D blocking antibody alleviated stroke outcome in terms of infarct volume and functional deficits, coinciding with reduced immune cell infiltration into the brain and improved survival in the animal model of cerebral ischemia. Using transgenic knockout models devoid of certain immune cell types and immunodeficient mice supplemented with different immune cell subsets, we dissected the functional contribution of NKG2D signaling by different NKG2D-expressing cells in stroke pathophysiology. The observed effect of NKG2D signaling in stroke progression was shown to be predominantly mediated by natural killer and CD8<sup>+</sup> T cells. Transfer of T cells with monovariant T-cell receptors into immunodeficient mice with and without pharmacological blockade of NKG2D revealed activation of CD8<sup>+</sup> T cells irrespective of antigen specificity. Detection of the NKG2D receptor and its ligands in brain samples of patients with stroke strengthens the relevance of preclinical observations in human disease.

**CONCLUSIONS:** Our findings provide a mechanistic insight into NKG2D-dependent natural killer- and T-cell-mediated effects in stroke pathophysiology.

**Key Words:** inflammation ■ middle cerebral artery occlusion ■ natural killer cells ■ NKG2D receptor ■ stroke

As one of the leading causes of long-term disabilities and death, stroke continues to be an enormous economic and social burden.<sup>1</sup> Accumulating evidence indicates that spatiotemporal dynamics of immune cell infiltration and subsequent immune responses contribute to secondary brain damage, neurodegeneration, and recovery after ischemic stroke.<sup>2,3</sup> T cell subsets in particular exacerbate stroke outcome, although natural killer (NK) cells have

been shown to contribute as well.<sup>4–6</sup> NK cells accumulate within infarct and peri-infarct areas as early as 3 hours after focal ischemia and propagate infarct size via cytotoxicity as well as cytokine and chemokine release.<sup>6,7</sup> Thereby, NK cells promote inflammation and recruit other immune cells to the brain, contributing to cerebral infarction.<sup>6,8,9</sup> However, the precise mechanisms underlying NK-cell-mediated stroke progression remain poorly understood.

Correspondence to: Christina David, MSc, Department of Neurology with C-TNBS, University Hospital Essen, Hufelandstraße 55, D-45147 Essen, Germany. Email: [christina.david@uk-essen.de](mailto:christina.david@uk-essen.de)

\*C. David, T. Ruck, S. G. Meuth, and C. Kleinschnitz contributed equally.

This article was sent to Neel S. Singhal, MD, PhD, Associate Editor, for review by expert referees, editorial decision, and final disposition.

Supplemental Material is available at <https://www.ahajournals.org/doi/suppl/10.1161/JAHA.122.029529>

For Sources of Funding and Disclosures, see page 13.

© 2023 The Authors. Published on behalf of the American Heart Association, Inc., by Wiley. This is an open access article under the terms of the [Creative Commons Attribution-NonCommercial](https://creativecommons.org/licenses/by-nc/4.0/) License, which permits use, distribution and reproduction in any medium, provided the original work is properly cited and is not used for commercial purposes.

JAHA is available at: [www.ahajournals.org/journal/jaha](http://www.ahajournals.org/journal/jaha)

## CLINICAL PERSPECTIVE

### What Is New?

- This study provides a mechanistic approach to natural killer- and T-cell function in ischemia-related brain damage and implicates the activating immune receptor NKG2D in early stroke development.
- NKG2D blockade was associated with improved stroke outcome and reduced immune cell infiltration into the ischemic brain.
- The observed effect of NKG2D signaling in the context of stroke was shown to be predominantly mediated by NK and CD8<sup>+</sup> T cells, independent of T-cell receptor signaling.

### What Are the Clinical Implications?

- Our findings contribute to a better understanding of the pathophysiology of ischemic stroke and point to a new therapeutic target in stroke therapy.

## Nonstandard Abbreviations and Acronyms

<b>LN</b>	lymph node
<b>MULT1</b>	murine UL16-binding protein-like transcript 1
<b>NRG</b>	NOD-Rag1 <sup>null</sup> IL2rg <sup>null</sup>
<b>RAE-1</b>	retinoic acid early transcript 1
<b>TCR</b>	T-cell receptor
<b>tMCAO</b>	transient middle cerebral artery occlusion
<b>ULBP</b>	cytomegalovirus UL16-binding protein
<b>WT</b>	wild-type

NK-cell activity depends on the balance of stimulatory and inhibitory signals; the latter can be overcome by the activating receptor NKG2D, which exerts effector function independent of inhibitory signals.<sup>10</sup> NKG2D is a c-type lectin-like NK immunoreceptor expressed on NK cells, natural killer T (NKT) cells, CD8<sup>+</sup>, and  $\gamma\delta$  T cells, as well as a subset of CD4<sup>+</sup> T cells.<sup>10–12</sup> The murine NKG2D receptor is characterized by two distinct isoforms that interact with different combinations of transmembrane adaptor proteins resulting in either cell-mediated cytotoxic responses or cytokine production.<sup>13–16</sup> However, the human receptor consists of only one isoform.<sup>17</sup>

NKG2D is involved in the regulation of effector functions of T cells and NK cells such as proliferation, migration, cytotoxicity, and cytokine production.<sup>18,19</sup> Three main types of ligands bind to the murine NKG2D receptor: histocompatibility H60 isoforms (H60a, b,

c),<sup>20</sup> retinoic acid early transcript 1 (RAE-1) isoforms  $\alpha$ ,  $\beta$ ,  $\gamma$ ,  $\delta$  and  $\epsilon$ ,<sup>21</sup> and murine UL16-binding protein-like transcript 1 (MULT1).<sup>22</sup> In the human system, major histocompatibility complex (MHC) class I chain-related proteins A/B<sup>10,23</sup> and 6 isoforms of cytomegalovirus UL16-binding proteins (ULBP1-6) have been identified as NKG2D ligands.<sup>24</sup>

Previous studies have demonstrated the importance of NKG2D signaling in autoimmune disorders such as multiple sclerosis<sup>19</sup> and in models of ischemia–reperfusion organ injury.<sup>25,26</sup> To evaluate the role of NKG2D signaling in stroke pathogenesis, we blocked NKG2D in mice subjected to transient middle cerebral artery occlusion (tMCAO), and analyzed stroke outcome and immune cell infiltration in the brain. To dissect the functional contribution of NKG2D signaling by different immune cell types, we transferred defined immune cell subsets into immunodeficient Rag1<sup>tm1Mom</sup> (Rag1<sup>-/-</sup>) mice devoid of mature T and B cells<sup>27</sup> and NOD-Rag1<sup>null</sup>IL2rg<sup>null</sup> (NRG) mice with a combined Rag1 and interleukin-2-receptor- $\gamma$  null mutation lacking mature T, B, and NK cells<sup>28</sup> before tMCAO, with or without NKG2D blockade. The role of NKG2D signaling in stroke pathophysiology for NKT and  $\gamma\delta$  T cells was investigated in transgenic knockout mouse models. To evaluate functional capacity of NKG2D-blocked immune cell subsets after stroke, surface exposure of the cytotoxicity marker CD107a on immune cells isolated from the ischemic brain of experimental animals was measured in a degranulation assay. Characterization of the NKG2D pathway in the context of stroke includes investigations of NKG2D ligand expression and localization in the murine and human brain. This work contributes to a better understanding of the complex pathophysiology of stroke and enables new opportunities for drug development.

## METHODS

### Availability of Data and Material

The data that support the findings of this study are available from the corresponding author upon reasonable request.

### Animals

C57BL/6N mice, purchased from Charles River Laboratories (Sulzfeld, Germany), served as control animals. Age and sex-matched NKG2D<sup>-/-</sup> (#022733), Rag1<sup>-/-</sup> (#002216), NRG (#007799), CD1d<sup>-/-</sup> (#008881),  $\gamma\delta$ <sup>-/-</sup> (#002120), OT-1 (#642), and OT-2 (#643) mice were purchased from Jackson Laboratories (Bar Harbor, ME) or Charles River Laboratories and were maintained in individually ventilated cages. We used mice of both sexes as donors

for adoptive transfer experiments, but only male mice were subjected to tMCAO to reduce variability of our results due to sex differences. Animals were excluded from end-point analyses if death occurred within 24 hours after tMCAO or exclusion criteria were reached, defined in a score that includes general conditions, spontaneous behavior, weight loss, and method-specific criteria, that is, Bederson score  $\geq 4$  or sustained score of 3. The number of excluded animals is given in [Table S1](#). Detailed information on the number of animals included in each experimental part is provided in [Figures 1-5](#), [Figures S1-S3](#), and in [Table S1](#). Animal experiments were approved by local authorities (Landesamt für Natur, Umwelt und Verbraucherschutz, North Rhine-Westphalia, Germany; Regierung von Unterfranken, Bavaria, Germany). All experiments were conducted following the ARRIVE guidelines including prespecified sample size and power calculations (80%; G\*Power 3.1.9.4.) and in accordance with the German laws and animal welfare regulations.

### Ischemia Model and Functional Outcome

Transient middle cerebral artery occlusion with the intraluminal filament technique induced focal cerebral ischemia in 10- to 12-week-old male mice as described previously.<sup>29</sup> Surgery and evaluation of all read-out parameters were performed in a blinded manner. Bederson score was applied to monitor global neurological impairments.<sup>30</sup> Grip test assessed motor function and coordination of experimental animals.<sup>31</sup>

### Measurements of Cerebral Infarct Volumes

Animals were euthanized via transcardial perfusion with PBS under anesthesia, and the removed brain was cut into 2-mm-thick coronal sections. To measure infarcted brain areas, brain slices were stained for 10 minutes at room temperature with 2% 2,3,5-triphenyltetrazolium chloride (Sigma-Aldrich, Burlington, MA).<sup>32</sup> Planimetric measurements (ImageJ software; National Institutes of Health) were used to calculate edema-corrected lesion volumes.

### NKG2D Blockade by anti-NKG2D Antibody

To pharmacologically block NKG2D receptor signaling, mice were injected intraperitoneally with 150  $\mu\text{g}$ <sup>19</sup> of NKG2D-specific monoclonal antibody or the respective control antibody. The blocking antibody and Rat immunoglobulin G1 isotype control antibody were purchased from eBioscience (San Diego, CA). The prophylactic group was treated 1 hour before tMCAO, whereas therapeutic treatment was

administered 1 hour and 3 hours after stroke. To ensure blockade of NKG2D signaling during the entire experiment in setups exceeding 24 hours, antibodies were administered every second day from stroke induction.

### Cell Isolation and Adoptive Transfer

Single-cell suspensions were prepared following standard protocols. Immunodeficient NRG mice were substituted with  $1 \times 10^7$  wild-type (WT) splenocytes and sacrificed before and 1 and 5 days after adoptive cell transfer.  $1 \times 10^6$  NK cells, CD4<sup>+</sup> T cells, and CD8<sup>+</sup> T cells were injected in recipient mice intravenously after in vitro preincubation with the anti-NKG2D and the control antibody for 1 hour. Further details are provided in [Data S1](#).

### Flow Cytometry

Brain, spleen, and lymph nodes (LNs) were isolated from PBS-perfused WT and NRG mice, and single-cell suspensions were prepared.  $1 \times 10^6$  cells were surface stained with fluorescence-labeled antibodies following standard protocols. Further details are given in [Data S1](#).

### Cytotoxicity Assay

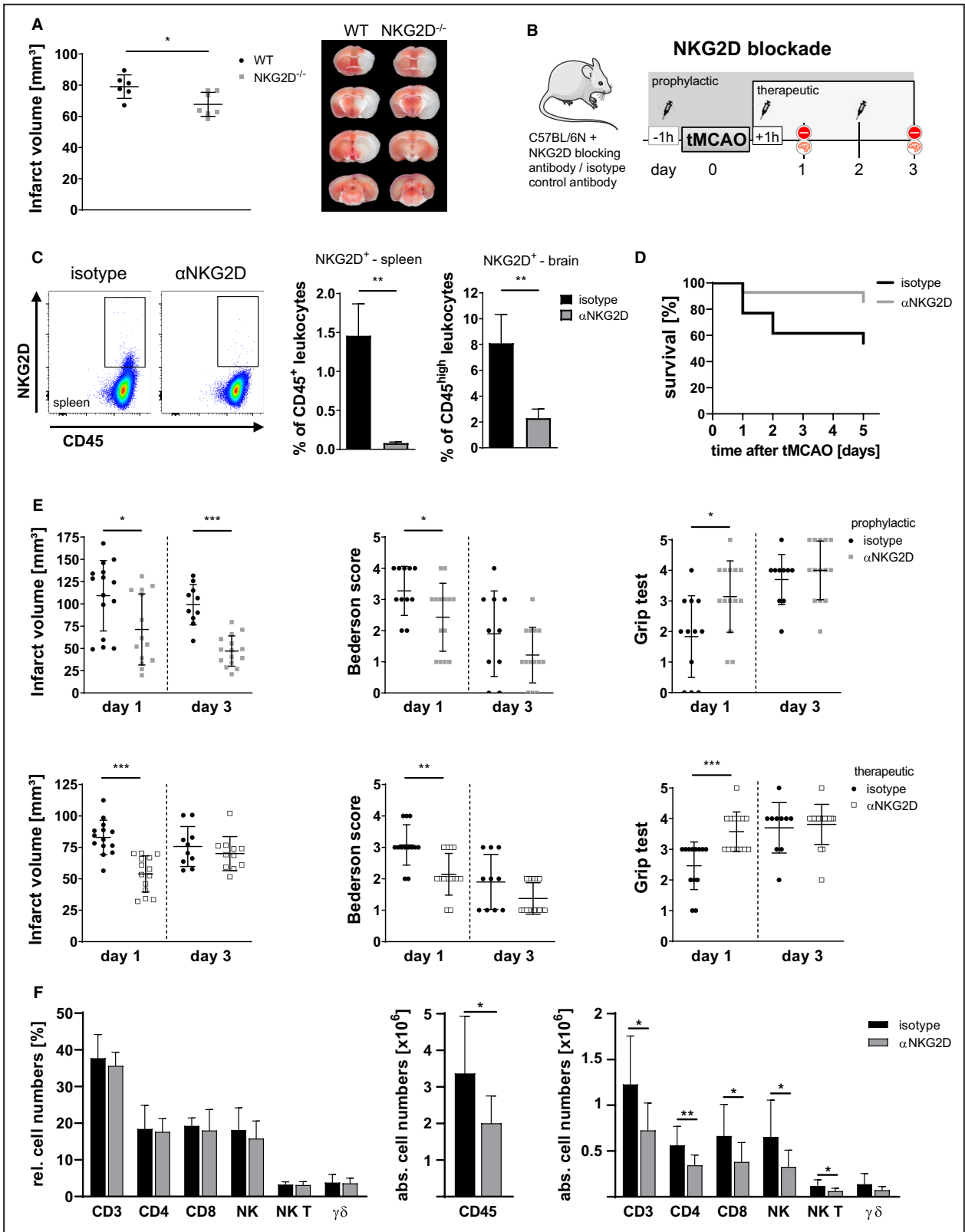
CD107a expression on NK cells and CD8<sup>+</sup> T cells isolated from  $\alpha\text{NKG2D}$  and isotype control treated animals 24 hours after tMCAO was measured to evaluate degranulation. Intracerebral leukocytes were isolated and stimulated with YAC-1 target cells at a ratio of 10:1 in the presence of CD107a antibody as well as the anti-NKG2D blocking antibody and the respective control antibody. The assay was incubated for 14 hours at 37°C/5%CO<sub>2</sub>. Cells were washed, stained, and analyzed using flow cytometry. Details on the fluorescently labeled antibodies are provided in [Data S1](#).

### RNA Isolation and Real-Time Polymerase Chain Reaction of NKG2D Ligands

RNA was isolated with the Quick-RNA Microprep Kit (Zymo Research, Germany) following the manufacturer's protocol. Details are provided in [Data S1](#).

### Immunofluorescence Staining of Human Brain Tissue

Human post-mortem brain tissue was obtained in accordance with the principles of the Declaration of Helsinki. Patients gave informed consent and the local ethics committee approved the study. Detailed staining protocols and clinical data for human samples are given in [Data S1](#) and in [Tables S2](#) and [S3](#).



### Statistical Analysis

Data presentation and all statistical analyses were performed with Prism software version 8 (GraphPad Software, La Jolla, CA). Data from the same condition

of individual tMCAO experiments were pooled for neurological scoring and infarct size measurements.

Statistical differences were determined by Student's *t*-test for normally distributed data and

**Figure 1. Pharmacological blockade of NKG2D signaling attenuates cerebral ischemia–reperfusion injury.**

**A**, Infarct volumes and representative TTC-stained brain slices from NKG2D<sup>-/-</sup> (n=7) and WT mice (n=6). **B**, Schematic illustration of the experimental protocol. Mice were treated prophylactically 1 hour before and therapeutically 1 hour after tMCAO with 150 µg of an anti-NKG2D blocking antibody and the respective isotype control. **C**, Confirmation of NKG2D receptor blockade by flow cytometric analysis of NKG2D<sup>+</sup> leukocytes in the spleen (ctr. n=4 vs αNKG2D n=6) and in the brain (ctr. n=5 vs αNKG2D n=5) of mice treated with NKG2D-blocking and control antibody. **D**, Kaplan–Meier survival plots of animals prophylactically treated with the anti-NKG2D antibody (n=14) compared with control group (n=13) up to 5 days after tMCAO surgery. **E**, Stroke outcome parameters in mice subjected to 60-minute tMCAO with prophylactic and therapeutic treatment with NKG2D-blocking antibody or isotype control. Infarct volumes, Bederson score, and grip test were evaluated 1 day (proph.: infarct volume ctr. n=15 vs αNKG2D n=14, scores ctr. n=11 vs αNKG2D n=14; ther.: infarct volume ctr. n=14 vs αNKG2D n=14, scores ctr. n=13 vs αNKG2D n=14) and 3 days after stroke induction (proph.: infarct volume ctr. n=10 vs αNKG2D n=15, scores ctr. n=10 vs αNKG2D n=14; ther.: infarct volume ctr. n=10 vs αNKG2D n=11, scores ctr. n=10 vs αNKG2D n=16). **F**, Relative and absolute numbers of brain infiltrating immune cell subsets of anti-NKG2D and isotype control antibody-treated WT mice 24 hours after stroke (ctr. n=10, αNKG2D n=12). NK indicates natural killer cell; NKT, natural killer T cell; tMCAO, transient middle cerebral artery occlusion; TTC, 2,3,5-triphenyltetrazolium chloride; and WT, wild-type.

a Mann–Whitney test for nonparametric data without normality and equality of variance. Post-stroke survival was plotted as Kaplan–Meier curve. The level of significance was labeled according to the *P* values (\**P*<0.05, \*\**P*<0.01, or \*\*\**P*<0.001). All results are given as mean±SD.

## RESULTS

### In Vivo Relevance of NKG2D Signaling in Early Stroke Progression

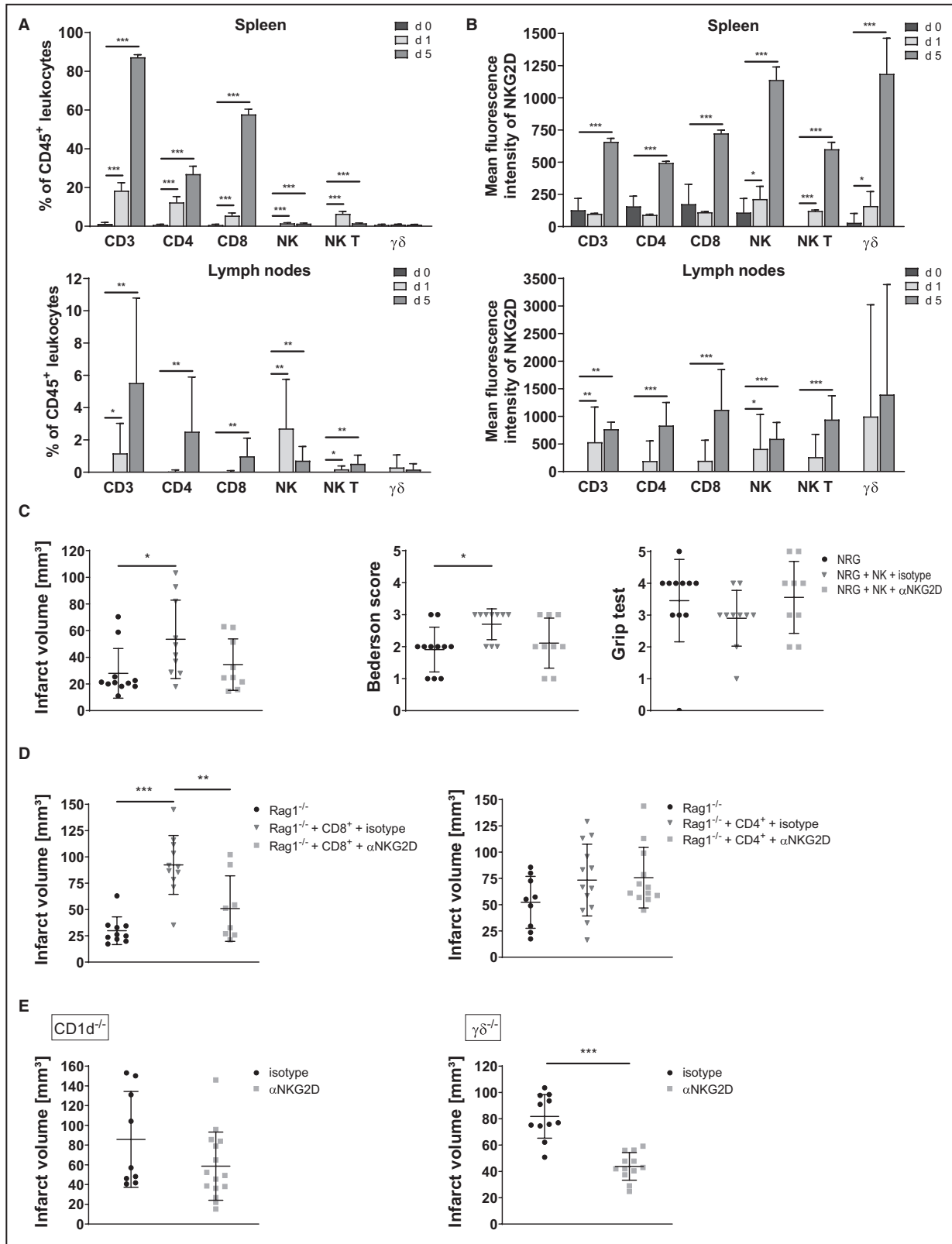
To evaluate the contribution of NKG2D receptor signaling in early stroke progression, WT and NKG2D<sup>-/-</sup> mice were subjected to tMCAO. In NKG2D<sup>-/-</sup> mice exons 1b–6 are globally knocked out, resulting in a lack of NKG2D expression, while the number of NK cells and other immune cell subsets remains normal.<sup>33</sup> Absent NKG2D receptor expression of NKG2D<sup>-/-</sup> mice was associated with smaller brain infarctions (Figure 1A, NKG2D<sup>-/-</sup>: 67.68 mm<sup>3</sup>±7.70 mm<sup>3</sup>, n=7 versus ctr.: 79.04 mm<sup>3</sup>±7.54 mm<sup>3</sup>, n=6, *P*=0.0215) and improved Bederson scores (Figure S1A, NKG2D<sup>-/-</sup>: 1.86±0.69, n=7 versus ctr.: 3±0.63, n=6, *P*=0.0103) compared with WT mice 24 hours after 60-minute tMCAO. Vessel density (CD31<sup>+</sup> vessels per mm<sup>2</sup>) was unchanged in these animals (Figure S1B, NKG2D<sup>-/-</sup>: 66±16 CD31<sup>+</sup> cells per mm<sup>2</sup>, n=4 versus ctr.: 90±21 CD31<sup>+</sup> cells per mm<sup>2</sup>, n=3, *P*=0.141).

Pharmacological blockade of the receptor was used to systematically assess impact of NKG2D blockade before and after stroke induction. WT mice were treated with an anti-NKG2D blocking antibody or the respective isotype control antibody according to the depicted injection scheme (Figure 1B). In the prophylactic treatment, 150 µg of blocking and isotype control antibodies were administered 1 hour before stroke induction, while in the therapeutic group the antibody was given 1 hour after stroke. In a pilot experiment, application intervals were tested to ensure the blockade of NKG2D signaling during experiments longer than 24 hours, resulting in antibody injections every second

day from stroke induction. Blockade of NKG2D receptor was confirmed 24 hours after antibody treatment by flow cytometry, gating for NKG2D<sup>+</sup> CD45<sup>+</sup> leukocytes in the spleen and for NKG2D<sup>+</sup> CD45<sup>high</sup> leukocytes in the brain (Figure 1C). Due to epitope masking by the blocking antibody, the proportion of NKG2D<sup>+</sup> leukocytes with a functional NKG2D receptor was significantly reduced in the spleen (αNKG2D: 0.08%±0.02%, n=6 versus ctr.: 1.46%±0.41%, n=4, *P*=0.0095) and the brain (αNKG2D: 2.29%±0.71%, n=5 versus ctr.: 8.10%±2.23%, n=5, *P*=0.0079) compared with control animals, while the proportion of CD49b<sup>+</sup> NK cells remained unchanged in the spleen (αNKG2D: 4.66%±0.48%, n=6 versus ctr.: 4.60%±0.38%, n=4, *P*=0.9143) and the brain (αNKG2D: 3.51%±0.41%, n=5 versus ctr.: 3.91%±0.34%, n=5, *P*=0.1508) upon NKG2D receptor blockade (Figure S1C).

Overall survival of anti-NKG2D-treated animals shown in a Kaplan–Meier plot was improved compared with the control group up to 5 days after tMCAO (Figure 1D, αNKG2D: n=14, ctr.: n=13). Prophylactic treatment of WT mice improved stroke outcome compared with isotype controls in terms of reduced infarct volumes (Figure 1E, αNKG2D: 71.27 mm<sup>3</sup>±39.87 mm<sup>3</sup>, n=14 versus ctr.: 109.1 mm<sup>3</sup>±39.51 mm<sup>3</sup>, n=15, *P*=0.0161) and Bederson scores (αNKG2D: 2.43±1.09, n=14 versus ctr.: 3.27±0.79, n=11, *P*=0.0494) as well as grip test scores (αNKG2D: 3.14±1.17, n=14 versus ctr.: 1.83±1.34, n=12, *P*=0.0145) 24 hours after stroke induction. Three days after focal cerebral ischemia, the effect of NKG2D blockade on stroke volume was even more pronounced (αNKG2D: 47.03 mm<sup>3</sup>±17.02 mm<sup>3</sup>, n=15 versus ctr.: 99.10 mm<sup>3</sup>±22.74 mm<sup>3</sup>, n=10, *P*<0.0001) but behavioral scores did not reach significance level (Bederson score: αNKG2D: 1.2±0.89, n=14 versus ctr.: 1.9±1.37, n=10, *P*=0.21; grip test: αNKG2D: 4.0±0.96, n=14 versus ctr.: 3.7±0.82, n=10, *P*=0.41).

Therapeutic NKG2D blockade resulted in a marked reduction of infarct volumes (Figure 1E, αNKG2D: 53.84 mm<sup>3</sup>±14.37 mm<sup>3</sup>, n=14 versus ctr.: 82.91 mm<sup>3</sup>±13.71 mm<sup>3</sup>, n=14, *P*<0.0001) and less severe neurological deficits (Bederson: 2.14±0.66; grip



test:  $3.57 \pm 0.65$ ,  $n=14$ ) compared with isotype control (Bederson:  $3.08 \pm 0.64$ ,  $P=0.0019$ ; grip test:  $2.46 \pm 0.78$ ,  $n=13$ ,  $P=0.0006$ ) 24 hours after tMCAO. Interestingly, however, 3 days after stroke induction, infarct volumes

( $\alpha$ NKG2D:  $70.04 \text{ mm}^3 \pm 13.51 \text{ mm}^3$ ,  $n=11$  versus ctr.:  $75.67 \text{ mm}^3 \pm 15.87 \text{ mm}^3$ ,  $n=10$ ,  $P=0.47$ ) and behavioral scores (Bederson score:  $\alpha$ NKG2D:  $1.38 \pm 0.50$ ,  $n=16$  versus ctr.:  $1.9 \pm 0.88$ ,  $n=10$ ,  $P=0.10$ ; grip test:

**Figure 2. Detrimental effect of NKG2D signaling is predominantly mediated by NK cells and CD8<sup>+</sup> T cells.**

Flow cytometric evaluation of immune cell composition (A) and NKG2D receptor distribution (B) on immune cell subsets in lymph nodes and spleen of immunodeficient NRG mice reconstituted with splenocytes before (n=6), 1 day after (n=8), and 5 days (n=8) after adoptive transfer. C, Stroke outcome parameters 24 hours after stroke induction in NRG mice reconstituted with isotype antibody-treated (n=10) and anti-NKG2D antibody-treated NK cells (n=9) prior to 60-minute tMCAO. NRG mice subjected to tMCAO served as control animals (n=11). D, Infarct volumes of naïve Rag1<sup>-/-</sup> mice after tMCAO (n=10, n=9) and animals that received preincubated NKG2D-blocked or isotype antibody-treated CD8<sup>+</sup> T cells (ctr. n=11 vs αNKG2D n=8) and CD4<sup>+</sup> T cells (ctr. n=13 vs αNKG2D n=12) prior to stroke induction. E, Infarct volumes of CD1d<sup>-/-</sup> mice, lacking NKT cells, and γδ<sup>-/-</sup> animals, devoid of γδ T cells, 24 hour after 60-minute tMCAO with and without blockade of NKG2D (CD1d<sup>-/-</sup>: ctr. n=9 vs αNKG2D n=15; γδ: ctr. n=11 vs αNKG2D n=12). NK indicates natural killer; NRG, NOD-Rag1<sup>nu/nu</sup>IL2rg<sup>nu/nu</sup>; and tMCAO, transient middle cerebral artery occlusion.

αNKG2D: 3.81±0.66, n=16 versus ctr.: 3.7±0.82, n=10,  $P=0.72$ ) were unchanged among these groups, indicating the NKG2D signaling cascade to be relevant in the very early response to ischemia. In an extended therapeutic window of 3 hours after stroke, NKG2D blockade resulted in infarct volumes and functional scores similar to the control group (Figure S2A, αNKG2D: 61.49mm<sup>3</sup>±12.22mm<sup>3</sup>, n=6 versus ctr.: 63.44mm<sup>3</sup>±8.46mm<sup>3</sup>, n=7,  $P=0.74$ ). Comparing relative cell numbers of infiltrated CD3<sup>+</sup> T cells, CD4<sup>+</sup> T helper cells, CD8<sup>+</sup> cytotoxic T cells, NK cells, NKT cells, and γδ T cells into the brain of WT animals 24 hours after stroke, blockade of NKG2D evoked no significant changes (αNKG2D: n=12, ctr.: n=10), but displayed a significant reduction of immune cell infiltration considering absolute cell numbers (Figure 1F, αNKG2D: n=12, ctr.: n=10). Thus, blockade of NKG2D signaling alleviated stroke outcome parameters, improved overall survival, and limited infiltration of immune cells into the brain of anti-NKG2D-treated animals.

### NK Cells and CD8<sup>+</sup> T Cells Are Drivers in NKG2D-Mediated Ischemic Brain Damage After Stroke

To confirm successful substitution of immunodeficient NRG mice with different immune cell subsets, we adoptively transferred splenocytes from WT mice into NRG mice and analyzed leukocyte subpopulations in LNs and spleen by flow cytometry at different time points (Figure 2A, d0: n=6, d1: n=8, d5: n=8). We could confirm successful transfer of NK cells, NKT cells, and CD3<sup>+</sup> T cells as well as CD8<sup>+</sup> and CD4<sup>+</sup> T-cell subsets into NRG mice. The proportion of most of these cell types increased compared with baseline within 1 day in spleen and LNs, which was even more pronounced by day 5. In LNs studied at day 1 after transfer, however, the increase of CD4<sup>+</sup> and CD8<sup>+</sup> T cells was modest and not statistically significant. Reconstitution with splenocytes was insufficient to elevate the frequency of the rare γδ T-cell population in both spleen and LNs 1 day and 5 days after adoptive transfer with regard to baseline.

To examine NKG2D receptor distribution on leukocyte subpopulations, we analyzed NKG2D expression in spleen and LNs before and 1 day and 5 days after reconstitution of NRG mice with splenocytes. While the

mean fluorescence intensity of NKG2D was unchanged on some immune cell populations 1 day after adoptive transfer, receptor expression was increased in all investigated immune cell subsets except for LN-derived γδ T cells 5 days after adoptive transfer (Figure 2B, d0: n=6, d1: n=8, d5: n=8).

The NKG2D receptor is expressed on NK cells, NKT cells, CD8<sup>+</sup> T cells, and γδ and a subset of CD4<sup>+</sup> T cells. To dissect functional implications of NKG2D signaling for different NKG2D expressing cells, we performed tMCAO in immunodeficient mice after adoptive transfer of different WT lymphoid cells with or without NKG2D blockade. NRG mice were reconstituted with NK cells incubated with anti-NKG2D blocking and isotype control antibody before cell transfer. Naïve NRG mice after tMCAO served as control animals. Adoptive transfer of NK cells preincubated with an isotype control antibody resulted in exacerbation of stroke outcome with regard to naïve control animals. Infarct volumes were significantly increased (Figure 2C, naïve: 27.96mm<sup>3</sup>±18.64mm<sup>3</sup>, n=11 versus ctr. AB: 53.50mm<sup>3</sup>±29.40mm<sup>3</sup>, n=10,  $P=0.019$ ) and animals performed worse in Bederson test assessing global neurological impairment (naïve: 1.91±0.70, n=11 versus ctr. AB: 2.70±0.48, n=10,  $P=0.0153$ ). The detrimental effect of isotype-treated NK cells was reversed by pharmacological blockade of NKG2D receptor signaling. Animals receiving NK cells with blocked NKG2D receptor signaling showed infarct sizes (34.51mm<sup>3</sup>±19.32mm<sup>3</sup>, n=9) and neurological scores (Bederson score: 2.11±0.78; grip test: 3.56±1.13, n=9) similar to those from control mice.

Rag1<sup>-/-</sup> mice devoid of mature T and B cells were reconstituted with CD8<sup>+</sup> T cells that were treated in vitro with anti-NKG2D blocking and isotype control antibodies before adoptive transfer. Naïve Rag1<sup>-/-</sup> mice after tMCAO served as control animals. Induction of focal ischemia in these animals revealed a significant reduction in infarct volumes compared with those of Rag1<sup>-/-</sup> mice reconstituted with isotype control pretreated CD8<sup>+</sup> T cells (Figure 2D, naïve: 29.86mm<sup>3</sup>±13.16mm<sup>3</sup>, n=10 versus ctr. AB: 92.36mm<sup>3</sup>±27.36mm<sup>3</sup>, n=11,  $P<0.0001$ ) as well as exacerbation of Bederson score and grip test scores (Figure S3A, Bederson: naïve: 1.80±0.79, n=10 versus ctr.: 3.09±0.54, n=11,  $P=0.0008$ ; grip test: naïve: 3.90±0.57, n=10 versus ctr.: 2.73±1.27, n=11,  $P=0.0006$ ). Adoptive transfer of CD8<sup>+</sup> cells preincubated with the

$\alpha$ NKG2D antibody reversed exacerbation of stroke outcome in terms of reduced infarct volumes ( $\alpha$ NKG2D:  $50.88\text{mm}^3 \pm 31.17\text{mm}^3$ ,  $n=8$ ,  $P=0.0073$ ) and improved grip test scores relative to isotype control group ( $\alpha$ NKG2D:  $3.50 \pm 0.55$ ,  $n=6$ ,  $P=0.0346$ ). However, anti-NKG2D antibody treatment of  $\text{CD4}^+$  T cells before transfer in  $\text{Rag1}^{-/-}$  mice was insufficient to reduce infarct volume volumes (Figure 2D, naïve:  $52.24\text{mm}^3 \pm 24.72\text{mm}^3$ ,  $n=9$  versus  $\alpha$ NKG2D:  $75.68\text{mm}^3 \pm 28.85\text{mm}^3$ ,  $n=12$  versus ctr.:  $73.38\text{mm}^3 \pm 34.14\text{mm}^3$ ,  $n=13$ ) or to improve global neurological deficits as well as motor function after focal cerebral ischemia (Figure S3A).

Additionally, we used knockout animals devoid of specific immune cell types in the presence of an NKG2D blocking antibody. In  $\text{CD1d}^{-/-}$  animals lacking NKT cells, administration of an anti-NKG2D blocking antibody did not affect stroke volume (Figure 2E,  $\alpha$ NKG2D:  $58.63\text{mm}^3 \pm 34.55\text{mm}^3$ ,  $n=15$  versus ctr.:  $85.82\text{mm}^3 \pm 48.56\text{mm}^3$ ,  $n=9$ ,  $P=0.138$ ) and functional scores (Figure S3B). In a knockout model devoid of  $\gamma\delta$  T cells, infarct volumes were reduced (Figure 2E,  $\alpha$ NKG2D:  $43.80\text{mm}^3 \pm 10.49\text{mm}^3$ ,  $n=12$  versus ctr.:  $81.82\text{mm}^3 \pm 16.52\text{mm}^3$ ,  $n=11$ ,  $P<0.0001$ ) and functional scores were improved by  $\alpha$ NKG2D antibody treatment (Figure S3B). Consequently, we demonstrated a role of NK cells and  $\text{CD8}^+$  T cells in NKG2D-mediated brain damage in the context of stroke.

### NKG2D-Mediated Activation of $\text{CD8}^+$ T Cells Is Independent of T-Cell Receptor Signaling and Acts Through Increased Cytotoxicity

The expression of NKG2D in  $\text{CD8}^+$  T cells depends on T cell receptor (TCR) activation.<sup>34</sup> To distinguish between TCR-dependent or -independent effects of

NKG2D activation for T cells in the context of stroke, we reconstituted  $\text{Rag1}^{-/-}$  mice with T cells from TCR transgenic mice (OT-1 and OT-2).  $\text{CD8}^+$  T cells from OT-1 mice and  $\text{CD4}^+$  T cells from OT-2 mice harbor a monovariant TCR that only recognizes ovalbumin and, in its absence, prevents TCR activation of these cells. Incubation of OT-1  $\text{CD8}^+$  T cells with anti-NKG2D antibody prior to adoptive transfer into  $\text{Rag1}^{-/-}$  mice resulted in smaller infarct volumes (Figure 3A,  $46.45\text{mm}^3 \pm 27.02\text{mm}^3$ ,  $n=8$ ,  $P=0.0112$ ) relative to the isotype control group ( $93.35\text{mm}^3 \pm 36.56\text{mm}^3$ ,  $n=8$ ) but was not able to ameliorate neurological scores (Figure S3C). However, adoptive transfer of OT-2  $\text{CD4}^+$  T cells with NKG2D-blockade before 60-minute tMCAO had no effect on infarct volume (Figure 3B,  $\alpha$ NKG2D:  $66.18\text{mm}^3 \pm 35.15\text{mm}^3$ ,  $n=9$  versus ctr.:  $72.07\text{mm}^3 \pm 27.56\text{mm}^3$ ,  $n=9$ ,  $P=0.387$ ) and functional scores (Figure S3C). Thus, activation of  $\text{CD8}^+$  T cells via the NKG2D receptor is independent of TCR signaling.

To address the mechanism mediating protective effects after NKG2D blockade, we evaluated functionality of NKG2D-blocked  $\text{CD8}^+$  T cells and NK cells after stroke by measuring the surface exposure of CD107a and thereby the release of cytotoxic granules in an in vitro cytotoxicity assay. After 60 minutes of tMCAO in anti-NKG2D and control antibody-treated WT animals, intracerebral leukocytes were isolated and in vitro stimulated with YAC-1 target cells in the presence of NKG2D blocking antibody and the respective isotype control antibody as well as anti-CD107a antibody. The analysis of CD107a as a marker for NK- and T-cell activation and cytotoxic degranulation revealed a significant decrease of CD107a expression on  $\text{CD8}^+$  T cells after NKG2D blockade (Figure 3C,  $49.05\% \pm 6.91\%$ ,  $n=4$ ) compared with control ( $63.03\% \pm 5.35\%$ ,  $n=7$ ,  $P=0.0061$ ). Comparing the proportion of CD107a<sup>+</sup> NK

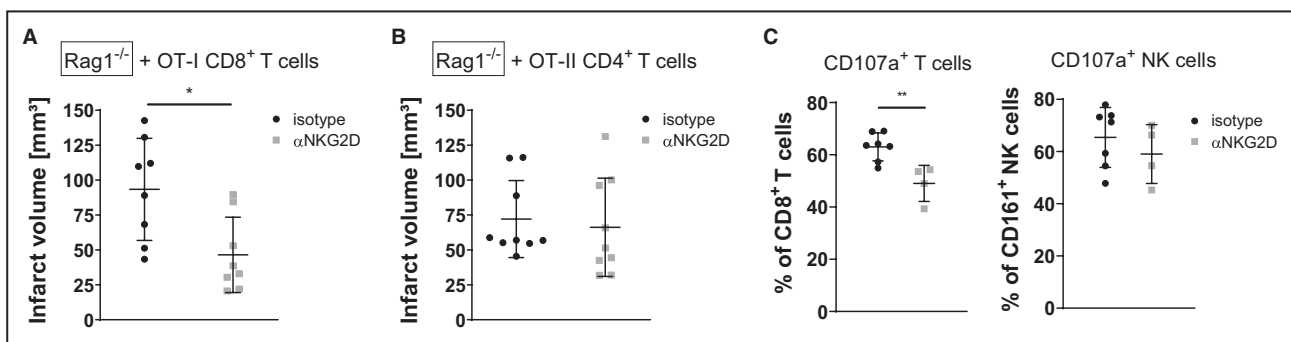


**Figure 3.** NKG2D signaling in  $\text{CD8}^+$  T cells is irrespective of antigen specificity in the context of ischemic stroke and mediates effects via increased cytotoxicity.

**A**, Infarct volumes were evaluated 24 hours after 60-minute tMCAO in  $\text{Rag1}^{-/-}$  mice reconstituted with  $\text{CD8}^+$  T cells derived from OT-1 mice and preincubated with anti-NKG2D blocking ( $n=8$ ) and control antibody ( $n=8$ ). **B**,  $\text{CD4}^+$  T cells, isolated from OT-2 mice, were incubated with isotype control ( $n=9$ ) and anti-NKG2D antibody ( $n=9$ ) before transfer into  $\text{Rag1}^{-/-}$  mice. Infarct volumes were assessed after 60-minute tMCAO. **C**, Proportion of  $\text{CD107a}^+$   $\text{CD8}^+$  T cells and NK cells, derived from anti-NKG2D ( $n=4$ ) and isotype antibody ( $n=7$ ) treated animals subjected to 60-minute tMCAO, and in vitro stimulated with YAC-1 target cells to assess cytolytic function. NK indicates natural killer; and tMCAO, transient middle cerebral artery occlusion.



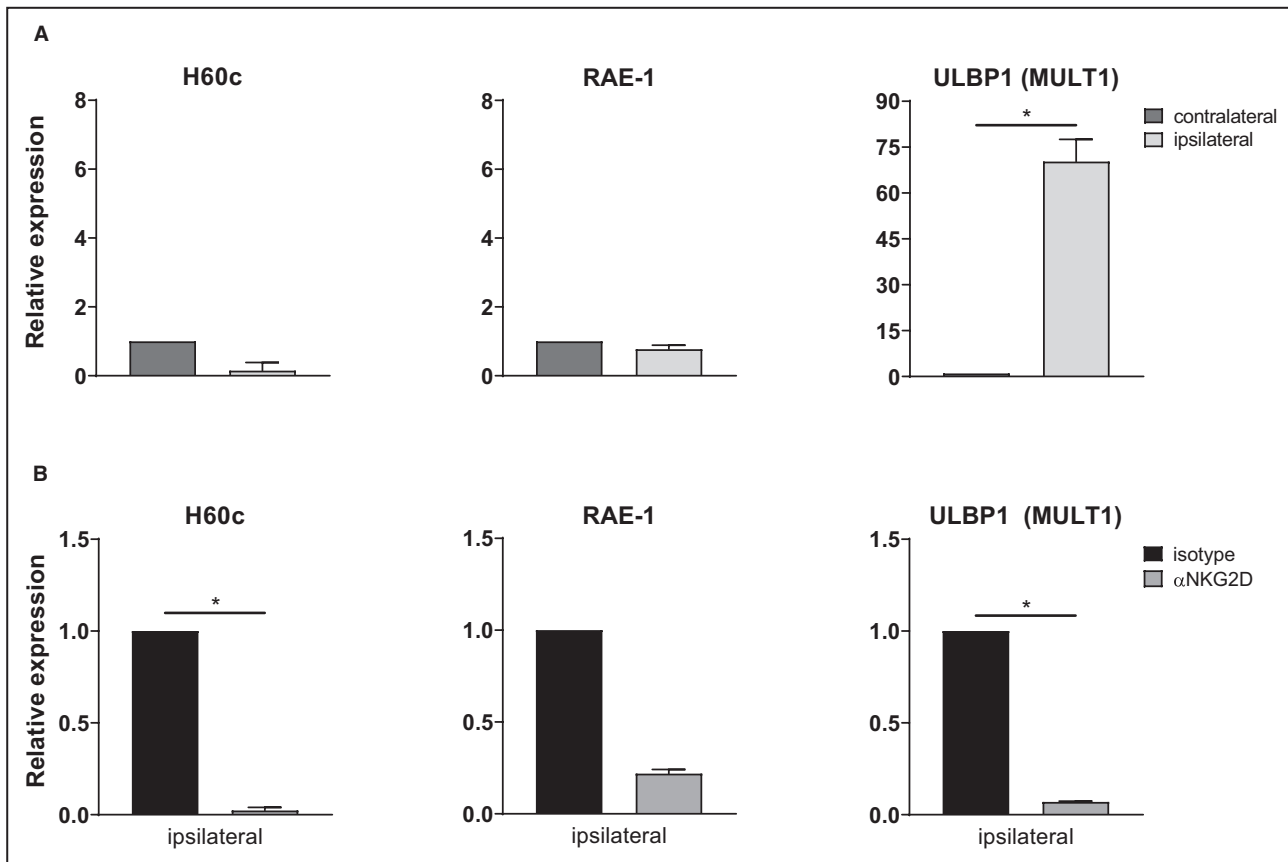


**Figure 4.** Expression of NKG2D ligands H60c, RAE-1, and ULBP1 (MULT1) in murine brain tissue after stroke.

**A**, Messenger RNA expression of H60c, RAE-1, and ULBP1 was analyzed by real-time polymerase chain reaction in brain lysates of WT mice 24 hours after stroke induction (n=4). **B**, Ipsilateral mRNA expression of H60c, RAE-1, and ULBP1 in brain lysates of WT mice treated with the anti-NKG2D blocking antibody (n=4) relative to ligand expression in the brain of isotype-treated animals (n=4) 24 hours after stroke surgery. MULT1: murine UL16-binding protein-like transcript 1; RAE-1: retinoic acid early transcript 1; ULBP: cytomegalovirus UL16-binding protein; and WT: wild-type.

cells after NKG2D blockade and isotype control antibody treatment, NK cells display no difference in cytolytic function in vitro ( $\alpha$ NKG2D:  $59.05\% \pm 11.27\%$ , n=4 versus ctr.:  $65.40\% \pm 11.46\%$ , n=7,  $P=0.40$ ).

### Regulation of NKG2D Ligand Expression in the Murine Brain After Focal Cerebral Ischemia

To identify interaction partners of NKG2D-expressing cells in stroke, we determined mRNA expression of NKG2D ligands in brain tissue of WT mice 24 hours after tMCAO. Expression of H60c, RAE-1, and ULBP1 (MULT1) in the ipsilateral hemisphere was normalized to contralateral ligand expression. While mRNA expression of H60c (Figure 4A,  $0.15 \pm 0.24$ ) and RAE-1 ( $0.77 \pm 0.12$ ) was unchanged among brain hemispheres, expression of the stress-inducible NKG2D ligand ULBP1 was significantly increased in ischemic cortices relative to contralateral expression ( $70.26 \pm 7.27$ ,  $P=0.024$ ). After pharmacological blockade of NKG2D signaling, mRNA expression in the ipsilateral cortices was normalized to

the expression in brain tissue of isotype control-treated animals. After blockade of NKG2D signaling, expression of H60c ( $0.02 \pm 0.02$ ,  $P=0.028$ ) and ULBP1 ( $0.07 \pm 0.005$ ,  $P=0.035$ ) was significantly reduced compared with isotype control, while RAE-1 expression in the ipsilateral brain hemisphere tended to be reduced without reaching statistical significance (Figure 4B,  $0.22 \pm 0.02$ ,  $P=0.11$ ).

### Relevance of NKG2D Signaling in Human Patients With Stroke

In post-mortem brain tissue from patients with ischemic stroke and control patients, we assessed the distribution of NKG2D-expressing immune cells. A higher abundance of NKG2D positivity was detected by histology of brains obtained from patients with stroke versus controls. Furthermore, infiltrated CD3<sup>+</sup> T cells, CD4<sup>+</sup> and CD8<sup>+</sup> T-cell subsets, CD56<sup>+</sup> NK cells and CD56<sup>+</sup>CD3<sup>+</sup> NKT cells were absent in the control brain. However, in stroke lesions, we found CD4<sup>+</sup> and CD8<sup>+</sup> T cells, NK cells, and NKT cells that expressed the NKG2D receptor (Figure 5A).

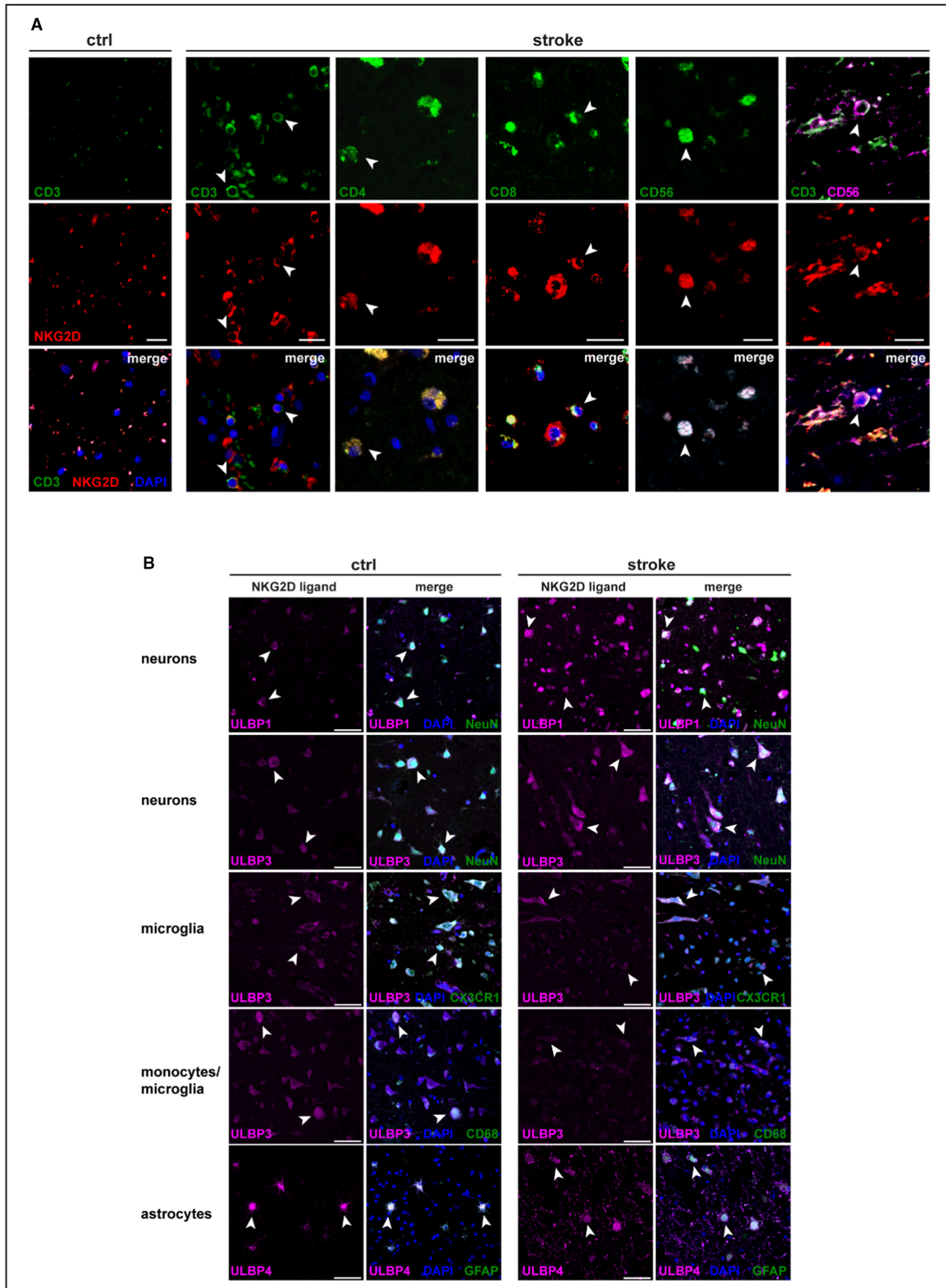


**Figure 5. Distribution of NKG2D-expressing immune cells and their interaction with ligand-expressing brain resident cells in human stroke patients.**

**A**, Representative immunofluorescence staining of NKG2D receptor as well as CD3<sup>+</sup> T cells, CD4<sup>+</sup> and CD8<sup>+</sup> T cell subsets, CD56<sup>+</sup> NK cells, and CD56<sup>+</sup>/CD3<sup>+</sup> NKT cells in the brain of human patients with stroke and control patients. **B**, Representative immunofluorescence staining of NKG2D ligands (ULBP1, -3, and -4) as well as NeuN<sup>+</sup> neurons, CX3CR1<sup>+</sup> microglia, CD68<sup>+</sup> monocytes/microglia, and glial fibrillary acidic protein (GFAP<sup>+</sup>) astrocytes in control brain tissue and stroke lesions. ULBP: cytomegalovirus UL16-binding protein. NK indicates natural killer cell; and NKT, natural killer T cell.

By colocalization studies of different markers for human NKG2D ligands (ULBP1, -3 and -4) and central nervous system resident astrocytes (glial fibrillary acidic protein), neurons (NeuN), monocytes/microglia (CD68), and microglial cells (CX3CR1), we identified predominant interactions partners in NKG2D signaling. NKG2D ligand expression was demonstrated in brain tissue of control as well as stroke patients (Figure 5B). NeuN<sup>+</sup> neurons express the NKG2D ligand ULBP1 and ULBP3, the latter is additionally expressed by CX3CR1<sup>+</sup> microglial cells and CD68<sup>+</sup> monocytes. ULBP4 was found to be coexpressed with the astrocytic marker glial fibrillary acidic protein.

## DISCUSSION

Early and delayed inflammatory processes are critically involved in stroke pathogenesis. Modulation of immune cells by depletion, systemic arrest, or impaired cerebral infiltration was shown to have a protective effect in the context of stroke.<sup>4,35–37</sup> Particularly, T and NK cells were demonstrated to contribute to stroke progression; however, underlying mechanisms remain poorly understood.<sup>4,5</sup> We now highlight the activating immunoreceptor NKG2D as a key mediator of T and NK cell-related effects in ischemia-related brain damage. Absent NKG2D receptor expression in NKG2D<sup>-/-</sup> mice and pharmacological blockade of NKG2D receptor signaling before stroke were associated with improved stroke outcome 24 hours and 3 days after tMCAO. Therapeutic anti-NKG2D antibody treatment improved stroke outcome 24 hours after tMCAO, but the effect was absent after 3 days. These results suggest that blocking NKG2D receptor signaling delayed, rather than prevented ischemic tissue damage. Blockade of the NKG2D receptor may possibly be compensated by activation of other stimulatory receptor pathways, such as the CD94/NKG2C receptor complex, or by restriction of inhibitory signaling. In the context of stroke, expression of a ligand for the inhibitory NKG2A receptor has been shown to be significantly reduced, suggesting loss of NK-cell tolerance<sup>6</sup> as another mechanism possibly involved in cerebral inflammation after ischemic injury.

In the extended therapeutic window of 3 hours after stroke, NKG2D blockade did not yield as consistent effects as in the 1-hour treatment group. The observed effects of NKG2D blockade were no longer present, suggesting that treatment in the 3-hour time window occurred too late to target early infiltrating immune cells. Kinetics of post-stroke inflammation demonstrated accumulation of NK and T cells in the ischemic tissue as early as 3 hours after stroke induction.<sup>6,38</sup> Therefore, these data further substantiate the relevance of the NKG2D signaling cascade in the early response to ischemia, at least in mice.

Numbers of brain-infiltrating immune cells are reduced after anti-NKG2D antibody treatment, indicating that NKG2D signaling influences inflammation after stroke. However, less immune cell infiltration into the ischemic brain may also have resulted from reduced infarct volumes. Our findings cannot prove causality of smaller infarct volumes and reduced cerebral immune cells infiltration but rather remain on a correlative level. However, the fact that infarct volumes are likewise smaller following adoptive transfer of pretreated NKG2D-blocked immune cells (Figure 2C and 2D) suggests a significant role of distinct immune cells in NKG2D-mediated stroke pathogenesis. Reduced leukocyte recruitment into the ischemic brain after NKG2D blockade is possibly related to reduced migratory capacity and less attraction of leukocytes into the brain since migration of CD4<sup>+</sup> T cells into the central nervous system was already shown to be limited by blockade of NKG2D signaling in experimental autoimmune encephalomyelitis (EAE), the animal model of multiple sclerosis.<sup>19</sup> In a model of cardiac ischemia, NKG2D blockade resulted in decreased expressions of proinflammatory cytokines such as tumor necrosis factor (TNF) and interleukin-17 and the intercellular adhesion molecule (ICAM),<sup>25</sup> which mediates transmigration of leukocytes across inflamed vascular endothelium into tissues.<sup>39</sup> NKG2D signaling and associated inflammatory processes might thus be involved in leukocyte recruitment to inflamed tissue.

As the receptor is expressed on a variety of immune cell subsets, we intended to identify those that contribute to the observed NKG2D-mediated effects by specifically targeting individual cell types. Reconstitution of NRG mice with NK cells and adoptive transfer of CD8<sup>+</sup> T cells in Rag1<sup>-/-</sup> mice without NKG2D-blockade before tMCAO resulted in larger infarct volumes, while they remained at baseline levels following reconstitution with NKG2D blocked cells. Thus, we were able to identify NK cells and CD8<sup>+</sup> T cells as essential mediators of NKG2D-related detrimental effects in the context of stroke. However, a possible impact of NK cells in Rag1<sup>-/-</sup> mice cannot be excluded. Nevertheless, any effect of NK cells would become equally visible in both NKG2D blocked and control antibody treated animals. Moreover, preincubation of adoptively transferred cells ensures targeting of NKG2D-mediated effects in CD8<sup>+</sup> and CD4<sup>+</sup> T cells.

CD4<sup>+</sup> T cells are not involved in NKG2D-mediated effects in stroke progression since NKG2D blockade in these cells failed to improve stroke outcome. However, in the context of autoimmune EAE, CD4<sup>+</sup> T cells were shown to be critically involved in development of inflammatory central nervous system lesions,<sup>19</sup> indicating the role of NKG2D<sup>+</sup> CD4<sup>+</sup> T cells to depend on the pathological conditions.

NKT and  $\gamma\delta$  T cells are rare cell populations, as demonstrated in our adoptive transfer experiments of

WT splenocytes into NRG mice. This is consistent with previous work, showing that NKT cells represent 0.2% to 2.5% of lymphocytes in the blood and lymphatic organs<sup>40</sup> and with 1% to 5% of circulating lymphocytes in the peripheral blood, the population of  $\gamma\delta$  T cells is a minor subset of T cells.<sup>41</sup> In our rodent stroke model, transgenic  $\gamma\delta^{-/-}$  knockout mice demonstrate significantly reduced stroke volumes after NKG2D blockade even though these animals are devoid of  $\gamma\delta$  T cells. This indicates that NKG2D-related effects in stroke are independent of  $\gamma\delta$  T cells and mediated by other immune cell subsets. We already identified NK cells and CD8<sup>+</sup> T cells to mediate stroke progression via NKG2D signaling, and these cells are still present in the knockout model, driving the observed effects after NKG2D blockade. Nonetheless, due to rarity of  $\gamma\delta$  T cells, an involvement of this cell population cannot be excluded. Sixty minutes of tMCAO causes severe cerebral damage that might override the pathophysiological contribution of less frequent cell populations. Previous work demonstrated absence of  $\gamma\delta$  T cells to play a protective role in stroke by ameliorating brain injury and diminishing inflammation. Interleukin-17 produced by  $\gamma\delta$  T cells was shown to recruit peripheral myeloid cells to the brain, thereby exacerbating ischemic brain damage.<sup>42</sup> Absence of NKT cells in CD1d<sup>-/-</sup> mice was associated with unchanged stroke outcome after NKG2D blockade, suggesting that NKT cells might be involved in NKG2D-related stroke progression. Adoptive transfer experiments with NKT and  $\gamma\delta$  T cells would have been more suitable to evaluate the contribution of these immune cell subsets but are not viable due to methodological limitations. The small number of cells would have led to an excessive number of donor animals, which is not compatible with the 3R rules (replacement, reduction, refinement). Additionally, viability of these cells after isolation via cell sorting was insufficient for adoptive transfer experiments.

Ligation of NKG2D can be directly stimulating or co-stimulatory, raising the question whether the observed NKG2D-related effects in stroke are depending on antigen specificity in different lymphocytic subpopulations. Activation of NKT cells and  $\gamma\delta$  T cells does not require classic antigen presentation. In general, NKT cells recognize antigens presented by the MHC class I-like protein CD1d, primarily expressed by antigen-presenting cells,<sup>43,44</sup> and once activated, they can kill target cells in a CD1d-dependent manner.<sup>45</sup> NKG2D ligation in NKT cells was shown to mediate both direct CD1d-independent lysis of target cells as well as co-stimulatory activation.<sup>46</sup> Instead, activation of CD8<sup>+</sup> and CD4<sup>+</sup> T cells usually requires co-stimulatory signals. NKG2D engagement in CD8<sup>+</sup> T cells was shown to act costimulatory and enhance TCR-mediated effector functions.<sup>18,34,47</sup> It has also been reported that under certain circumstances, considering the activation

status of the cell, these cells are directly activated by NKG2D without the contribution of the TCR.<sup>18</sup> In stroke pathogenesis, detrimental effects of CD8<sup>+</sup> T cells were shown to be independent of both TCR specificity and costimulation via CD28 and programmed cell death protein 1, but an underlying mechanism remained unknown.<sup>4,34</sup> Using genetically modified T cells with a TCR specifically binding to one predefined antigen (ovalbumin), our results demonstrate that exacerbating effects of CD8<sup>+</sup> T cells in cerebral ischemia mediated by NKG2D signaling are irrespective of antigen specificity and non-MHC restricted. We further demonstrated decreased cytotoxicity of CD8<sup>+</sup> T cells after NKG2D blockade since the expression of CD107a as a marker for degranulation<sup>48</sup> is reduced in an in vitro cytotoxicity assay. The diminished cytolytic function indicates a less inflammatory phenotype of NKG2D-blocked CD8<sup>+</sup> T cells. Together with the fact that no additional stimulation of the TCR is required for cell activation, this emphasizes the relevance of NKG2D signaling in CD8<sup>+</sup> T cells. However, NKG2D blockade did not change degranulation of NK cells in vitro in the context of stroke. Further studies on a potential NKG2D-mediated effect on cytokine production in NK cells are needed.

We further investigated the regulation of NKG2D ligand expression in the murine brain after stroke since differential expression of these ligands in normal tissue and pathological conditions is known.<sup>49,50</sup> An elevated level of NKG2D ligand expression is able to override signals of class I-mediated NK inhibition, proving ligand expression to be an important variable in NKG2D signaling.<sup>10,51</sup> Expression of ULBP1 was highly increased in the ischemic cortices indicating facilitated receptor-ligand interactions while H60c and RAE-1 expression were unchanged. Consistent with these findings, ULBP1 (MULT1) was shown to be significantly upregulated in the central nervous system of EAE mice at the peak of disease, and RAE-1 and H60 were modestly or not altered at mRNA level.<sup>52</sup> However, in a model of renal ischemia-reperfusion injury, H60 and ULBP1 (MULT1) expression were not detectable in renal tubular epithelial cells, while RAE-1 was elevated revealing ligand expression to depend on a variety of factors such as cell type and environment.<sup>26</sup> Multiple studies implied MULT1 to exhibit unique properties among all ligands for NKG2D since MULT1 binds the receptor with high affinity and shows a wider expression pattern than other ligands.<sup>22</sup> This indicates, together with our results, a broader role of ULBP1 (MULT1) in the context of stroke. Interestingly, H60c and ULBP1 were reduced in the ischemic hemisphere after NKG2D blockade, suggesting reduced cellular stress in the brain tissue of experimental animals since abundance of NKG2D ligands is generally low in healthy tissues but increases upon stress signals.<sup>49,50</sup> The reduced infarct volumes after receptor blockade are associated

with limited immune cell infiltration that might in turn result in less cellular stress.

Our results obtained in mice might also be of relevance in the human system. While the NKG2D receptor is only barely detectable in the brain of control patients, we demonstrated its expression on CD8<sup>+</sup> and CD4<sup>+</sup> T cells, NKT cells, and NK cells in brain tissue of stroke patients. Ligands of the NKG2D receptor were detected in both the control brain tissue and stroke lesions. While neurons express ULBP1, ULBP4 was solely colocalized with astrocytes and ULBP3 was found on neurons, monocytes, and microglia. Usually, the human ligands ULBP1-4 are known to be upregulated upon stress signals,<sup>53</sup> indicating a certain stress level in the control brains of our patients as well. These samples were taken from patients with no known pre-existing stroke, but we cannot exclude increased stress levels in control brain tissue. Overall, translation of our results to the clinics must be critically assessed due to limitations of the animal model. To reduce heterogeneity of our results, we used the standardized stroke model of tMCAO that is established in young male mice. Further studies with female mice as well as aged and comorbid animals reflecting aspects of the primarily affected elderly patients are needed. However, this study is a mechanistic proof-of-principle study rather than a translational approach, which would necessarily require these additional experimental conditions.

Our findings provide for the first time a mechanistic insight in the role of NKG2D in NK and CD8<sup>+</sup> T cell-mediated stroke progression. In both cell types, engagement of NKG2D mediates a strong stimulatory signal since the receptor is able to overcome inhibitory signals in NK cells<sup>10</sup> and does not require costimulation of the TCR to activate CD8<sup>+</sup> T cells in the context of stroke. Expression of the NKG2D receptor on relevant immune cell subsets in murine and human stroke pathophysiology strengthens the relevance of the pre-clinical observations for the human disease. NKG2D signaling is a complex and versatile pathway that acts as a master regulator of immune cell activation<sup>54</sup> and along with the possibility of pharmacological modulation, NKG2D and the associated pathway represent a promising treatment target. In conclusion, this work contributes to a better understanding of the complex immune pathophysiology of stroke and might provide new opportunities for drug development.

## ARTICLE INFORMATION

Received February 1, 2023; accepted April 4, 2023.

### Affiliations

Department of Neurology With Center for Translational Neuro- and Behavioral Sciences (C-TNBS), University Hospital Essen, University Duisburg-Essen, Essen, Germany (C.D., S.M., F.L., A.K.M., C.K.); Department of Neurology, Medical Faculty, Heinrich-Heine-University, Düsseldorf, Germany (T.R., L.R., C.B.S., R.J., S.G.M.); Department of Neurology, Hospital Main-Spessart,

Lohr am Main, Germany (P.K.); Department of Neurology, University Hospital Würzburg, Würzburg, Germany (P.K., M.K.S.); and Department of Pharmacology, University Hospital Essen, University of Duisburg-Essen, Essen, Germany (A.C.F.).

### Acknowledgments

The authors thank Steffi Hezel and Kristina Wagner for excellent technical support.

### Sources of Funding

This study was supported by research funding from Deutsche Forschungsgemeinschaft to Drs Meuth and Kleinschnitz (418901501) and to Drs Langhauser and Kleinschnitz (FOR-2879, 428778684), and by the Interdisciplinary Center for Clinical Research of the medical faculty of Münster to Dr Rolles (SEED-10/18).

### Disclosures

None.

### Supplemental Material

Data S1  
Tables S1–S3  
Figures S1–S3

## REFERENCES

- Johnson CO, Nguyen M, Roth GA, Nichols E, Alam T, Abate D, Abd-Allah F, Abdelalim A, Abraha HN, Abu-Rmeileh NM, et al. Global, regional, and national burden of stroke, 1990–2016: a systematic analysis for the global burden of disease study 2016. *Lancet Neurol*. 2019;18:439–458. doi: 10.1016/S1474-4422(19)30034-1
- Magnus T, Wiendl H, Kleinschnitz C. Immune mechanisms of stroke. *Curr Opin Neurol*. 2012;25:334–340. doi: 10.1097/WCO.0b013e328352ede6
- Gelderblom M, Leypoldt F, Steinbach K, Behrens D, Choe CU, Siler DA, Arumugam TV, Orthey E, Gerloff C, Tolosa E, et al. Temporal and spatial dynamics of cerebral immune cell accumulation in stroke. *Stroke*. 2009;40:1849–1857. doi: 10.1161/STROKEAHA.108.534503
- Kleinschnitz C, Schwab N, Kraft P, Hagedorn I, Dreykluft A, Schwarz T, Austinat M, Nieswandt B, Wiendl H, Stoll G. Early detrimental T-cell effects in experimental cerebral ischemia are neither related to adaptive immunity nor thrombus formation. *Blood*. 2010;115:3835–3842. doi: 10.1182/blood-2009-10-249078
- Rolles L, Ruck T, David C, Mencl S, Bock S, Schmidt M, Strecker JK, Pfeuffer S, Mecklenbeck AS, Gross C, et al. Natural killer cells are present in Rag1(−/−) mice and promote tissue damage during the acute phase of ischemic stroke. *Transl Stroke Res*. 2022;13:197–211. doi: 10.1007/s12975-021-00923-3
- Gan Y, Liu Q, Wu W, Yin JX, Bai XF, Shen R, Wang Y, Chen J, La Cava A, Poursine-Laurent J, et al. Ischemic neurons recruit natural killer cells that accelerate brain infarction. *Proc Natl Acad Sci USA*. 2014;111:2704–2709. doi: 10.1073/pnas.1315943111
- Zhang Y, Gao Z, Wang D, Zhang T, Sun B, Mu L, Wang J, Liu Y, Kong Q, Liu X, et al. Accumulation of natural killer cells in ischemic brain tissues and the chemotactic effect of IP-10. *J Neuroinflammation*. 2014;11:79. doi: 10.1186/1742-2094-11-79
- Seifert HA, Leonardo CC, Hall AA, Rowe DD, Collier LA, Benkovic SA, Willing AE, Pennypacker KR. The spleen contributes to stroke induced neurodegeneration through interferon gamma signaling. *Metab Brain Dis*. 2012;27:131–141. doi: 10.1007/s11011-012-9283-0
- Yilmaz G, Arumugam TV, Stokes KY, Granger DN. Role of T lymphocytes and interferon-gamma in ischemic stroke. *Circulation*. 2006;113:2105–2112. doi: 10.1161/CIRCULATIONAHA.105.593046
- Bauer S, Groh V, Wu J, Steinle A, Phillips JH, Lanier LL, Spies T. Activation of NK cells and T cells by NKG2D, a receptor for stress-inducible MICA. *Science*. 1999;285:727–729. doi: 10.1126/science.285.5428.727
- Yabe T, McSherry C, Bach FH, Fisch P, Schall RP, Sondel PM, Houchins JP. A multigene family on human chromosome 12 encodes natural killer-cell lectins. *Immunogenetics*. 1993;37:455–460. doi: 10.1007/BF00222470
- Ogasawara K, Lanier LL. NKG2D in NK and T cell-mediated immunity. *J Clin Immunol*. 2005;25:534–540. doi: 10.1007/s10875-005-8786-4
- Diefenbach A, Tomasello E, Lucas M, Jamieson AM, Hsia JK, Vivier E, Raulet DH. Selective associations with signaling proteins determine

- stimulatory versus costimulatory activity of NKG2D. *Nat Immunol.* 2002;3:1142–1149. doi: 10.1038/ni858
14. Wu J, Song Y, Bakker AB, Bauer S, Spies T, Lanier LL, Phillips JH. An activating immunoreceptor complex formed by NKG2D and DAP10. *Science.* 1999;285:730–732. doi: 10.1126/science.285.5428.730
  15. Gilfillan S, Ho EL, Cella M, Yokoyama WM, Colonna M. Nkg2d recruits two distinct adaptors to trigger NK cell activation and costimulation. *Nat Immunol.* 2002;3:1150–1155. doi: 10.1038/ni857
  16. Zompi S, Hamerman JA, Ogasawara K, Schweighoffer E, Tybulewicz VL, Di Santo JP, Lanier LL, Colucci F. NKG2D triggers cytotoxicity in mouse NK cells lacking DAP12 or Syk family kinases. *Nat Immunol.* 2003;4:565–572. doi: 10.1038/ni930
  17. Wu J, Chervinski H, Spies T, Phillips JH, Lanier LL. DAP10 and DAP12 form distinct, but functionally cooperative, receptor complexes in natural killer cells. *J Exp Med.* 2000;192:1059–1068. doi: 10.1084/jem.192.7.1059
  18. Verneris MR, Karimi M, Baker J, Jayaswal A, Negrin RS. Role of NKG2D signaling in the cytotoxicity of activated and expanded CD8+ T cells. *Blood.* 2004;103:3065–3072. doi: 10.1182/blood-2003-06-2125
  19. Ruck T, Bittner S, Gross CC, Breuer J, Albrecht S, Korr S, Gobel K, Pankratz S, Henschel CM, Schwab N, et al. CD4+NKG2D+ T cells exhibit enhanced migratory and encephalitogenic properties in neuroinflammation. *PLoS One.* 2013;8:e81455. doi: 10.1371/journal.pone.0081455
  20. Takada A, Yoshida S, Kajikawa M, Miyatake Y, Tomaru U, Sakai M, Chiba H, Maenaka K, Kohda D, Fugo K, et al. Two novel NKG2D ligands of the mouse H60 family with differential expression patterns and binding affinities to NKG2D. *J Immunol.* 2008;180:1678–1685. doi: 10.4049/jimmunol.180.3.1678
  21. Cerwenka A, Bakker AB, McClanahan T, Wagner J, Wu J, Phillips JH, Lanier LL. Retinoic acid early inducible genes define a ligand family for the activating NKG2D receptor in mice. *Immunity.* 2000;12:721–727. doi: 10.1016/S1074-7613(00)80222-8
  22. Carayannopoulos LN, Naidenko OV, Fremont DH, Yokoyama WM. Cutting edge: murine UL16-binding protein-like transcript 1: a newly described transcript encoding a high-affinity ligand for murine NKG2D. *J Immunol.* 2002;169:4079–4083. doi: 10.4049/jimmunol.169.8.4079
  23. Bahram S, Bresnahan M, Geraghty DE, Spies T. A second lineage of mammalian major histocompatibility complex class I genes. *Proc Natl Acad Sci USA.* 1994;91:6259–6263. doi: 10.1073/pnas.91.14.6259
  24. Cosman D, Mullberg J, Sutherland CL, Chin W, Armitage R, Fanslow W, Kubin M, Chalupny NJ. ULBPs, novel MHC class I-related molecules, bind to CMV glycoprotein UL16 and stimulate NK cytotoxicity through the NKG2D receptor. *Immunity.* 2001;14:123–133. doi: 10.1016/S1074-7613(01)00095-4
  25. Shen B, Li J, Yang B. NKG2D blockade significantly attenuates ischemia-reperfusion injury in a cardiac transplantation model. *Transplant Proc.* 2013;45:2513–2516. doi: 10.1016/j.transproceed.2013.02.126
  26. Zhang ZX, Wang S, Huang X, Min WP, Sun H, Liu W, Garcia B, Jevnikar AM. NK cells induce apoptosis in tubular epithelial cells and contribute to renal ischemia-reperfusion injury. *J Immunol.* 2008;181:7489–7498. doi: 10.4049/jimmunol.181.11.7489
  27. Mombaerts P, Iacomini J, Johnson RS, Herrup K, Tonegawa S, Papaioannou VE. RAG-1-deficient mice have no mature B and T lymphocytes. *Cell.* 1992;68:869–877. doi: 10.1016/0092-8674(92)90030-G
  28. Pearson T, Shultz LD, Miller D, King M, Laning J, Fodor W, Cuthbert A, Burzenski L, Gott B, Lyons B, et al. Non-obese diabetic-recombination activating gene-1 (NOD-Rag1 null) interleukin (IL)-2 receptor common gamma chain (IL2r gamma null) null mice: a radioresistant model for human lymphohaematopoietic engraftment. *Clin Exp Immunol.* 2008;154:270–284. doi: 10.1111/j.1365-2249.2008.03753.x
  29. Gob E, Reymann S, Langhauser F, Schuhmann MK, Kraft P, Thielmann I, Gobel K, Brede M, Homola G, Solymosi L, et al. Blocking of plasma kallikrein ameliorates stroke by reducing thromboinflammation. *Ann Neurol.* 2015;77:784–803. doi: 10.1002/ana.24380
  30. Bederson JB, Pitts LH, Tsuji M, Nishimura MC, Davis RL, Bartkowski H. Rat middle cerebral artery occlusion: evaluation of the model and development of a neurologic examination. *Stroke.* 1986;17:472–476. doi: 10.1161/01.STR.17.3.472
  31. Moran PM, Higgins LS, Cordell B, Moser PC. Age-related learning deficits in transgenic mice expressing the 751-amino acid isoform of human beta-amyloid precursor protein. *Proc Natl Acad Sci USA.* 1995;92:5341–5345. doi: 10.1073/pnas.92.12.5341
  32. Bederson JB, Pitts LH, Germano SM, Nishimura MC, Davis RL, Bartkowski HM. Evaluation of 2,3,5-triphenyltetrazolium chloride as a stain for detection and quantification of experimental cerebral infarction in rats. *Stroke.* 1986;17:1304–1308. doi: 10.1161/01.STR.17.6.1304
  33. Guerra N, Tan YX, Joncker NT, Choy A, Gallardo F, Xiong N, Knoblaugh S, Cado D, Greenberg NM, Raulet DH. NKG2D-deficient mice are defective in tumor surveillance in models of spontaneous malignancy. *Immunity.* 2008;28:571–580. doi: 10.1016/j.immuni.2008.02.016
  34. Groh V, Rhinehart R, Randolph-Habecker J, Topp MS, Riddell SR, Spies T. Costimulation of CD8alphabeta T cells by NKG2D via engagement by MIC induced on virus-infected cells. *Nat Immunol.* 2001;2:255–260. doi: 10.1038/85321
  35. Kraft P, Gob E, Schuhmann MK, Gobel K, Deppermann C, Thielmann I, Herrmann AM, Lorenz K, Brede M, Stoll G, et al. Fty720 ameliorates acute ischemic stroke in mice by reducing thrombo-inflammation but not by direct neuroprotection. *Stroke.* 2013;44:3202–3210. doi: 10.1161/STROKEAHA.113.002880
  36. Liesz A, Zhou W, Mracsko E, Karcher S, Bauer H, Schwarting S, Sun L, Bruder D, Stegemann S, Cerwenka A, et al. Inhibition of lymphocyte trafficking shields the brain against deleterious neuroinflammation after stroke. *Brain.* 2011;134:704–720. doi: 10.1093/brain/awr008
  37. Zhang RL, Chopp M, Li Y, Zaloga C, Jiang N, Jones ML, Miyasaka M, Ward PA. Anti-ICAM-1 antibody reduces ischemic cell damage after transient middle cerebral artery occlusion in the rat. *Neurology.* 1994;44:1747–1751. doi: 10.1212/WNL.44.9.1747
  38. Schuhmann MK, Bieber M, Franke M, Kollikowski AM, Stegner D, Heinze KG, Nieswandt B, Pham M, Stoll G. Platelets and lymphocytes drive progressive penumbral tissue loss during middle cerebral artery occlusion in mice. *J Neuroinflammation.* 2021;18:46. doi: 10.1186/s12974-021-02095-1
  39. Yang L, Froio RM, Sciuto TE, Dvorak AM, Alon R, Luscinckas FW. ICAM-1 regulates neutrophil adhesion and transcellular migration of TNF-alpha-activated vascular endothelium under flow. *Blood.* 2005;106:584–592. doi: 10.1182/blood-2004-12-4942
  40. van Puijvelde GHM, Kuiper J. NKT cells in cardiovascular diseases. *Eur J Pharmacol.* 2017;816:47–57. doi: 10.1016/j.ejphar.2017.03.052
  41. Carding SR, Egan PJ. Gammadelta T cells: functional plasticity and heterogeneity. *Nat Rev Immunol.* 2002;2:336–345. doi: 10.1038/nri797
  42. Shichita T, Sugiyama Y, Ooboshi H, Sugimori H, Nakagawa R, Takada I, Iwaki T, Okada Y, Iida M, Cua DJ, et al. Pivotal role of cerebral interleukin-17-producing gammadelta T cells in the delayed phase of ischemic brain injury. *Nat Med.* 2009;15:946–950. doi: 10.1038/nm.1999
  43. Exley M, Garcia J, Balk SP, Porcelli S. Requirements for CD1d recognition by human invariant Valpha24+ CD4-CD8- T cells. *J Exp Med.* 1997;186:109–120. doi: 10.1084/jem.186.1.109
  44. Blumberg RS, Terhorst C, Bleicher P, McDermott FV, Allan CH, Landau SB, Trier JS, Balk SP. Expression of a nonpolymorphic MHC class I-like molecule, CD1d, by human intestinal epithelial cells. *J Immunol.* 1991;147:2518–2524. doi: 10.4049/jimmunol.147.8.2518
  45. Wingender G, Krebs P, Beutler B, Kronenberg M. Antigen-specific cytotoxicity by invariant NKT cells in vivo is CD95/CD178-dependent and is correlated with antigenic potency. *J Immunol.* 2010;185:2721–2729. doi: 10.4049/jimmunol.1001018
  46. Kuylensstierna C, Bjorkstrom NK, Andersson SK, Sahlstrom P, Bosnjak L, Paquin-Proulx D, Malmberg KJ, Ljunggren HG, Moll M, Sandberg JK. NKG2D performs two functions in invariant NKT cells: direct TCR-independent activation of NK-like cytotoxicity and co-stimulation of activation by CD1d. *Eur J Immunol.* 2011;41:1913–1923. doi: 10.1002/eji.200940278
  47. Jamieson AM, Diefenbach A, McMahon CW, Xiong N, Carlyle JR, Raulet DH. The role of the NKG2D immunoreceptor in immune cell activation and natural killing. *Immunity.* 2002;17:19–29. doi: 10.1016/S1074-7613(02)00333-3
  48. Aktas E, Kucuksezzer UC, Bilgic S, Erten G, Deniz G. Relationship between CD107A expression and cytotoxic activity. *Cell Immunol.* 2009;254:149–154. doi: 10.1016/j.cellimm.2008.08.007
  49. Groh V, Bahram S, Bauer S, Herman A, Beauchamp M, Spies T. Cell stress-regulated human major histocompatibility complex class I gene expressed in gastrointestinal epithelium. *Proc Natl Acad Sci USA.* 1996;93:12445–12450. doi: 10.1073/pnas.93.22.12445
  50. Zou Z, Nomura M, Takihara Y, Yasunaga T, Shimada K. Isolation and characterization of retinoic acid-inducible cDNA clones in F9 cells: a

- 
- novel cDNA family encodes cell surface proteins sharing partial homology with MHC class I molecules. *J Biochem.* 1996;119:319–328. doi: [10.1093/oxfordjournals.jbchem.a021242](https://doi.org/10.1093/oxfordjournals.jbchem.a021242)
51. Cerwenka A, Baron JL, Lanier LL. Ectopic expression of retinoic acid early inducible-1 gene (RAE-1) permits natural killer cell-mediated rejection of a MHC class I-bearing tumor in vivo. *Proc Natl Acad Sci USA.* 2001;98:11521–11526. doi: [10.1073/pnas.201238598](https://doi.org/10.1073/pnas.201238598)
52. Legroux L, Moratalla AC, Laurent C, Deblois G, Verstraeten SL, Arbour N. NKG2D and its ligand MULT1 contribute to disease progression in a mouse model of multiple sclerosis. *Front Immunol.* 2019;10:154. doi: [10.3389/fimmu.2019.00154](https://doi.org/10.3389/fimmu.2019.00154)
53. Borchers MT, Harris NL, Wesselkamper SC, Vitucci M, Cosman D. NKG2D ligands are expressed on stressed human airway epithelial cells. *Am J Physiol Lung Cell Mol Physiol.* 2006;291:L222–L231. doi: [10.1152/ajplung.00327.2005](https://doi.org/10.1152/ajplung.00327.2005)
54. Wensveen FM, Jelencic V, Polic B. NKG2D: a master regulator of immune cell responsiveness. *Front Immunol.* 2018;9:441. doi: [10.3389/fimmu.2018.00441](https://doi.org/10.3389/fimmu.2018.00441)

# **Supplemental Material**



## **Data S1.**

### **Supplemental Methods**

#### *Animals*

Of the 451 mice subjected to tMCAO, 62 mice (13.7%) met at least one exclusion criteria after randomization and were therefore withdrawn from the study. In total, 473 animals were included in this study. Detailed information on the number of excluded animals is provided in Table S1.

#### *Cell isolation*

Brain, spleen, and lymph nodes (LN) from intracardially PBS-perfused WT and NRG mice were isolated and single-cell suspensions were prepared. Brain tissue was dissociated into single-cell suspensions using the Multi Tissue Dissociation Kit 1 (Miltenyi Biotec, Germany) in combination with the gentleMACS™ Octo Dissociator with heaters (Miltenyi Biotec, Germany) according to the provided protocol. Briefly, the dissected brain was homogenized in C-Tubes containing enzyme mix in the gentleMACS Octo Dissociator using program 37C\_Multi\_F. Debris and myelin were removed using the Debris Removal Solution.

Spleen and lymph nodes were strained through a 40-µm nylon filter (BD Biosciences, Germany). After ammonium chloride-based erythrocyte lysis with Pharm Lyse lysing buffer (BD Biosciences, Germany) homogenates were resuspended in PBS (Gibco Life Technologies, USA) containing 2% FBS, hereinafter referred to as staining buffer.

#### *Adoptive transfer experiments*

Immunodeficient NRG mice were substituted with WT splenocytes. Single cell suspension was prepared as described before and  $1 \times 10^7$  cells resuspended in PBS were injected intravenously in NRG mice. Leukocyte-reconstituted NRG mice were sacrificed before, 1 and 5 days after the adoptive cell transfer. Spleen and LN were analyzed by flow cytometry to confirm success of the cell transfer up to 5 days after transfer. The control group received PBS without splenocytes (day 0).

NK cells, CD4<sup>+</sup> T cells, and CD8<sup>+</sup> T cells were isolated from spleen and LN cell suspensions of WT mice. The different immune cell subsets were enriched by magnetic bead-based cell separation (NK cell isolation kit, CD4<sup>+</sup> T cell isolation kit, CD8<sup>+</sup> T cell isolation kit, Miltenyi Biotec, Germany) according to the supplier's manual prior

to flow cytometric cell sorting. Purity of  $\geq 90\%$  was achieved in all experiments. NK cells, CD4<sup>+</sup> T cells, and CD8<sup>+</sup> T cells were treated *in vitro* for 1 hour with the anti-NKG2D blocking antibody (CX5; 10 $\mu$ g/ml) and the respective Rat IgG1 isotype control antibody (eBRG1). 1 x 10<sup>6</sup> NK cells resuspended in PBS were injected intravenously by tail vein injection in NRG mice. Rag1<sup>-/-</sup> mice were reconstituted with 1 x 10<sup>6</sup> CD4<sup>+</sup> and CD8<sup>+</sup> T cells in PBS. 24 hours after injection, reconstituted NRG or Rag1<sup>-/-</sup> mice and control animals were exposed to 60-minutes tMCAO.

OT-I CD8<sup>+</sup> T cells and OT-II CD4<sup>+</sup> T cells with transgenic ovalbumin-specific T cell receptors were isolated from spleen and LN cell suspensions of OT-I and OT-II mice by MACS column-based isolation method using the CD8<sup>+</sup> and CD4<sup>+</sup> T cell isolation kit (Miltenyi Biotec, Germany) according to the supplier's manual. Adoptive transfer of 1 x 10<sup>6</sup> T cells in PBS was performed intravenously by tail vein injection in Rag1<sup>-/-</sup> mice after 1-hour preincubation with the blocking anti-NKG2D antibody and the respective isotype control. T cell-reconstituted Rag1<sup>-/-</sup> mice were subjected to tMCAO 24h after injection.

The control group received PBS without cells. NK cells, CD4<sup>+</sup> T cells, and CD8<sup>+</sup> T cells were analyzed for purity prior to transfer.

#### *Flow cytometry*

1 x 10<sup>6</sup> cells were surface stained for 30 min at 4°C with the appropriate combination of indicated fluorescence-labeled monoclonal antibodies in staining buffer following standard protocols. Fluorescence of cells was measured using a MACSQuant® Analyzer 10 Flow Cytometer (Miltenyi Biotec, Germany), a BD FACS Calibur Flow Cytometer (BD Biosciences), a Gallios Flow Cytometer (Beckman Coulter), or a BD FACS Aria III Cell Sorter (BD Biosciences, Germany) with BD FACS Diva 8.0 software (BD Biosciences, Germany). Frequencies of leukocyte subsets were analyzed with FlowJo 10.0 (LLC, OR, USA) or Kaluza Analysis Software (Beckman Coulter) and are referred to the CD45<sup>+</sup> leukocyte gate. NKG2D receptor expression was depicted as the mean fluorescence intensity. The following murine fluorescently labeled antibodies were used: CD45 (30-F11, Cat. 103116), CD3 (17A2, Cat. 100204), CD4 (RM4-5, Cat. 100531), CD8 (53-6.7, Cat. 100752), TCR  $\gamma/\delta$  (GL3, Cat. 118118), CD49b (DX5, Cat. 108908), NKG2D (CX5, Cat. 130212), CD161 (PK136, Cat. 108722; all BioLegend, CA, USA) and CD335 (29A1.4, 25-3351-82; Invitrogen, MA, USA). In the degranulation assay, the following fluorescently labeled antibodies purchased from Miltenyi Biotec were used: CD3 (17A2, Cat. 130-118-849), CD45 (REA737, Cat. 130-110-803), CD8a (REA601, Cat. 130-120-822), NKG2D (CX5, Cat. 130-102-730), CD107a (REA777, Cat. 130-111-505), CD161 (REA1162, Cat. 130-120-510).

#### *RNA isolation and real-time quantitative PCR (qPCR) of NKG2D ligands*

RNA was isolated with the Quick-RNA Microprep Kit (Zymo Research, Germany) following the manufacturer's protocol. Tissue homogenates and cells were lysed in RNA Lysis buffer, followed by sample clearing. The supernatant was mixed with 95-100% ethanol and in-column DNase treatment was performed. RNA was eluted by pre-warmed DNase/RNase-free water (15 µl). RNA quality was measured with Nanodrop by A260/A280 and A260/A230 ratios.

Reverse transcription was performed with Maxima Reverse Transcriptase (Thermo scientific, Germany) and hexamer primers. Following this, 100 ng cDNA was used for realtime qPCR with TaqMan Master Mix (Maxima probe/ROX; Applied Biosystem, Germany). To this end, 1 µM of each primer (target primers: murine H60c, Mm04243526\_m1; murine RAE-1, Mm00558293\_g1; murine MULT-1, Mm01180648\_m1; Thermo scientific, Germany) or 1 µM housekeeping primer for the respective control (18s, #4333760T), 10 µl of maxima probe/carboxyrhodamine (ROX) fluorescent dye, 4µl of DNA-free aqua and 100 ng cDNA (4µl) were mixed. Run was performed on a StepOnePlus™ Real-Time PCR System (Applied Biosystems, Germany) according to the following steps: hold - 2 min 50°C, initial denaturation - 10 min 95°C, amplification - (40x) 10 s 95°C - 45 s 58°C - 1 min 72°C. Data were analyzed with the StepOne software (Applied Biosystems, v2.1) calculating relative expression levels of H60c, RAE-1, and MULT-1 in the ipsilateral hemisphere by normalization to the contralateral ligand expression. In one set of experiments, expression levels in ipsilateral brain tissue of blocking antibody-treated mice were normalized to ligand expression in ipsilateral brain tissue of control antibody-treated animals.

#### *Immunofluorescence staining of NKG2D-expressing cells and NKG2D ligands*

Human post-mortem brain tissue was obtained in accordance with the principles of the Declaration of Helsinki and the local Ethics Committee approved the study. In Table S2 and S3, details on patient data and origin of the brain samples are provided.

Paraffin-embedded human brain tissue was sectioned into 5µm thick slices, deparaffinized and rehydrated. Sections were heated in citrate buffer for antigen retrieval, rinsed in PBS and incubated for 1 hour in 5% BSA in PBS to prevent unspecific antibody binding prior to incubation with following primary antibodies: anti-CD3 (1:50; MCA1477, Bio-Rad), anti-CD4 (1:100; MAB3706, Millipore), anti-CD8 (1:50; MA1-80231, Thermo Scientific), anti-NKG2D (1:200; ab89807, abcam and 1:100; ab203353, abcam), anti-CD56 (1:200; RBK050, Zytomed), anti-ULBP1 (1:50; MAB1380, R&D Systems), anti-ULBP3 (1:50; MAB1517, R&D Systems), anti-ULBP4 (1:50;

MAB6285, R&D Systems), anti-NeuN (1:250; ab177487, abcam), anti-GFAP (1:1000; 13-0300, Invitrogen), anti-CX3CR1 (1:100; ab8021, abcam) and anti-CD68 (1:100; PA5-32330, Invitrogen). Primary antibodies incubated overnight at 4 °C. Secondary antibodies conjugated with Alexa Fluor 488, Alexa Fluor 555, and Alexa Fluor 647 (1:250; Invitrogen) were applied in combination with DAPI (Sigma) for nuclear counterstaining and slides incubated for 1.5 hours at room temperature. Images were taken with a fluorescence microscope (Leica DMI8; Leica-Microsystems, Germany) and processed with ImageJ, Adobe Photoshop, or Illustrator.

**Table S1. Excluded animals for each experimental group.**

Animals	Treatment	Treatment timing	Ischemia Model	Experiment Duration	Excluded Animals	Figure
C57BL/6 WT	-	-	tMCAO	24 h	1 of 7	1A + S1A
NKG2D KO	-	-			0 of 7	
C57BL/6N WT	isotype ctr.	prophylactic	tMCAO	24 h	0 of 5	1C brain
C57BL/6N WT	$\alpha$ NKG2D				0 of 5	1C brain
C57BL/6N WT	isotype ctr.	prophylactic	tMCAO	5 days	0 of 13 (survial curve)	1D
C57BL/6N WT	$\alpha$ NKG2D				0 of 14 (survial curve)	
C57BL/6N WT	isotype ctr.	prophylactic	tMCAO	24 h	4 of 19	1C spleen + 1E
C57BL/6N WT	$\alpha$ NKG2D				2 of 16	
C57BL/6N WT	isotype ctr.	prophylactic	tMCAO	72 h	4 of 14	1C spleen + 1E
C57BL/6N WT	$\alpha$ NKG2D				2 of 17	
C57BL/6N WT	isotype ctr.	therapeutic	tMCAO	24 h	6 of 20	1E
C57BL/6N WT	$\alpha$ NKG2D				6 of 20	
C57BL/6N WT	isotype ctr.	therapeutic	tMCAO	72 h	2 of 12	1E
C57BL/6N WT	$\alpha$ NKG2D				1 of 12	
C57BL/6N WT	isotype ctr.	prophylactic	tMCAO	24 h	2 of 12	1F
C57BL/6N WT	$\alpha$ NKG2D				1 of 13	
NRG	-	-	-	0 h (baseline)	0 of 6	2A+B
NRG	AT splenocytes	-		24 h	0 of 8	
NRG	AT splenocytes	-		5 days	0 of 8	
NRG	-	-	tMCAO	24 h	1 of 12	2C
NRG	AT NK cells + isotype ctr.	pre-incubation			0 of 10	
NRG	AT NK cells + $\alpha$ NKG2D	pre-incubation			1 of 10	
Rag1 KO	-	-	tMCAO	24 h	0 of 10	2D
Rag1 KO	AT CD8 <sup>+</sup> T cells + isotype ctr.	pre-incubation			2 of 13	
Rag1 KO	AT CD8 <sup>+</sup> T cells + $\alpha$ NKG2D	pre-incubation			2 of 10	
Rag1 KO	-	-	tMCAO	24 h	1 of 10	2D
Rag1 KO	AT CD4 <sup>+</sup> T cells + isotype ctr.	pre-incubation			2 of 15	
Rag1 KO	AT CD4 <sup>+</sup> T cells + $\alpha$ NKG2D	pre-incubation			1 of 13	
CD1d KO	isotype ctr.	pre-incubation	tMCAO	24 h	1 of 10	2E
CD1d KO	$\alpha$ NKG2D				3 of 18	
$\gamma\delta$ KO	isotype ctr.	pre-incubation	tMCAO	24 h	1 of 12	2E
$\gamma\delta$ KO	$\alpha$ NKG2D				0 of 12	
Rag1 KO	AT OT-1 CD8 <sup>+</sup> T cells + isotype ctr.	pre-incubation	tMCAO	24 h	2 of 10	3A
Rag1 KO	AT OT-1 CD8 <sup>+</sup> T cells + $\alpha$ NKG2D				2 of 10	
Rag1 KO	AT OT-2 CD4 <sup>+</sup> T cells + isotype ctr.	pre-incubation	tMCAO	24 h	1 of 10	3B
Rag1 KO	AT OT-2 CD4 <sup>+</sup> T cells + $\alpha$ NKG2D				4 of 13	

C57BL/6N WT	isotype ctr.	prophylactic	tMCAO	24 h	1 of 8	3C
C57BL/6N WT	$\alpha$ NKG2D				1 of 5	
C57BL/6N WT	-	-	tMCAO	24 h	0 of 4	4A
C57BL/6N WT	-	-			0 of 4	
C57BL/6N WT	isotype ctr.	prophylactic	tMCAO	24 h	0 of 4	4B
C57BL/6N WT	$\alpha$ NKG2D				0 of 4	
C57BL/6N WT	isotype ctr.	therapeutic 3 h	tMCAO	24 h	3 of 10	S2A
C57BL/6N WT	$\alpha$ NKG2D				2 of 8	

**Table S2. Details on control patients.**

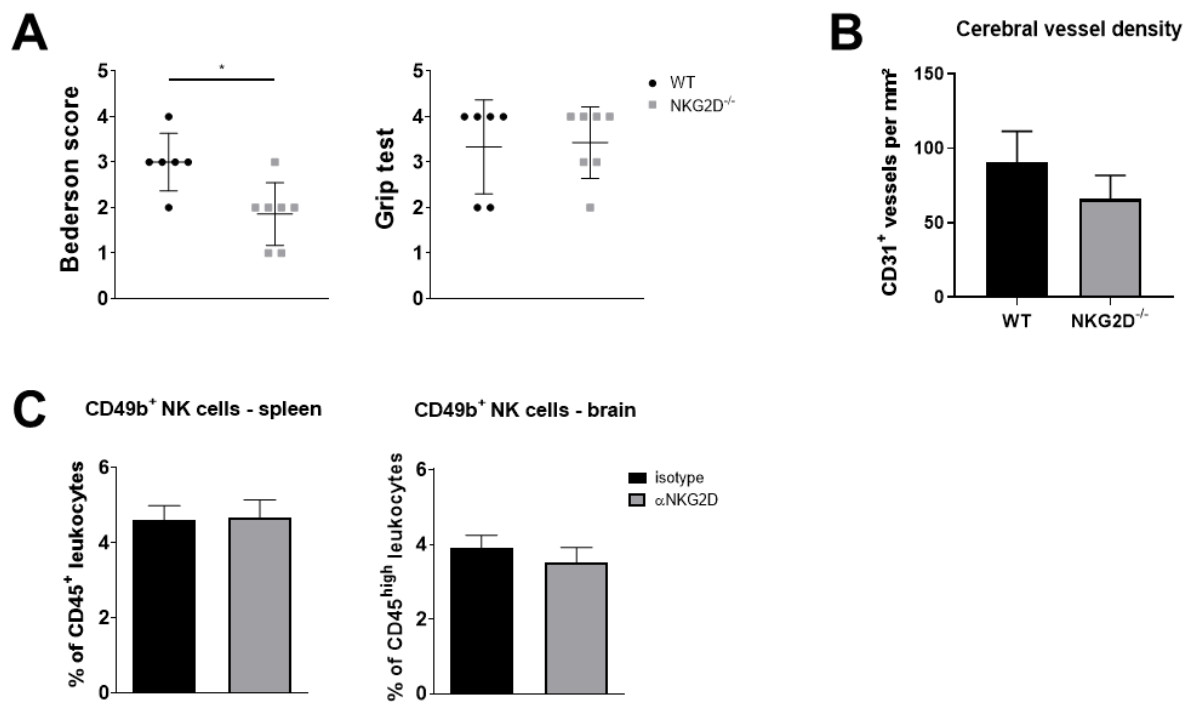
	age [years]	sex	neurologically relevant pre-existing diseases	cause of death
patient1	59	♂	none known	cardiogenic shock
patient2	69	♀	none known	septic shock, multi-organ failure
patient3	76	♂	none known	cardiogenic shock

**Table S3. Details on stroke patients and tissue origin.**

	age [years]	sex	time after stroke	stroke etiology	anatomical brain region	location of the sample
patient 1	68	♂	14 days	embolic	territory of A. cerebri media, parietal left	infarct area, parietal left
patient 2	57	♂	2 years	embolic	territory of A. cerebri media, temporal-parietal right	infarct area, temporal- parietal right

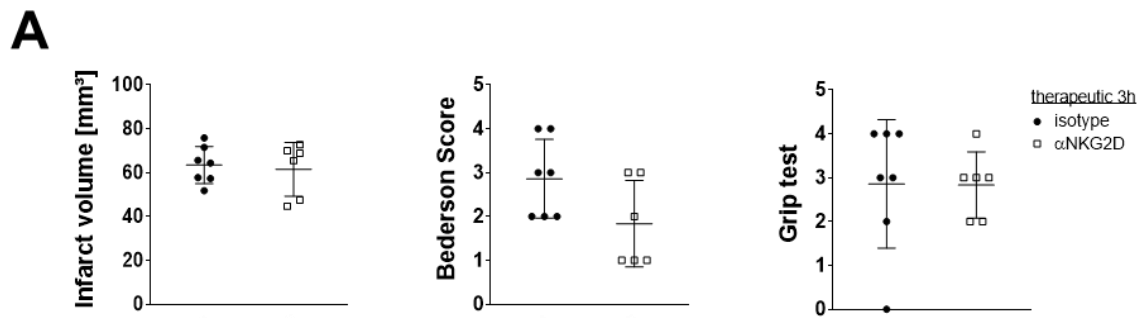


Figure S1. Functional stroke outcome and cerebral vessel density in WT and NKG2D<sup>-/-</sup> mice after stroke.



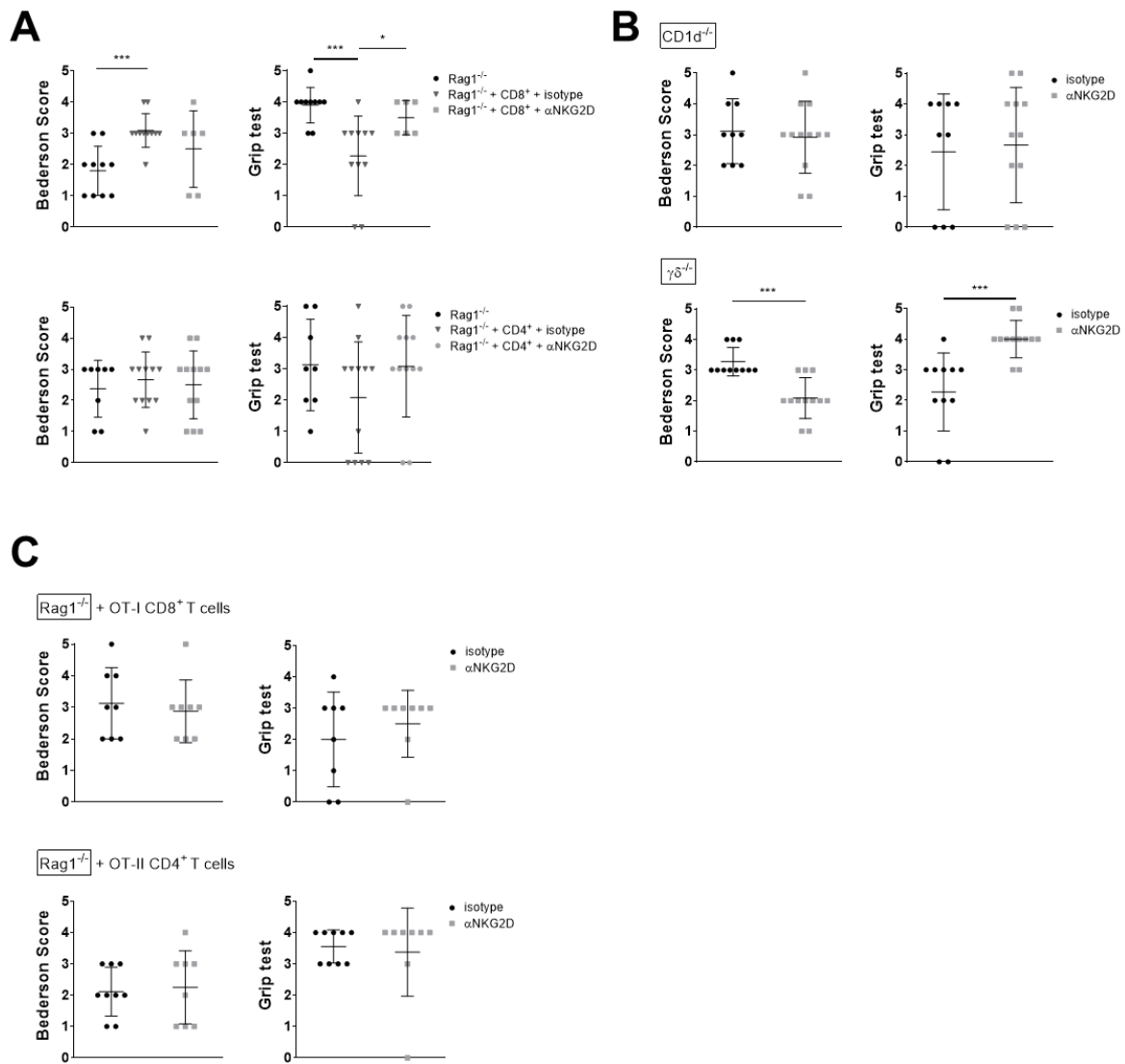
(A) Global neurological deficits (Bederson score) and motor function (grip test) of NKG2D<sup>-/-</sup> (n=7) and WT mice (n=6) 24h after tMCAO. (B) Numbers of CD31<sup>+</sup> vessels per mm<sup>2</sup> in the brain of WT (n=3) and NKG2D<sup>-/-</sup> mice (n=4) after 60-minutes tMCAO. (C) Relative numbers of CD49b<sup>+</sup> NK cells in the spleen and in the brain of anti-NKG2D and isotype control antibody-treated WT mice 24h after stroke (spleen: ctr. n=4 vs. αNKG2D n=6; brain: ctr. n=5 vs. αNKG2D n=5). tMCAO: transient middle cerebral artery occlusion; WT: wildtype

**Figure S2. Stroke outcome after pharmacological blockade of NKG2D signaling in an extended 3-hour time window after stroke induction.**



(A) Infarct volumes and functional scores of WT mice treated 3h post-stroke with isotype control (n=7) and αNKG2D antibody (n=6), evaluated 24h after 60-minutes tMCAO. tMCAO: transient middle cerebral artery occlusion; WT: wildtype

**Figure S3. Functional stroke outcome of adoptive transfer and transgenic animal models after NKG2D signaling blockade.**



(A) Functional stroke outcome of naïve Rag1<sup>-/-</sup> mice and animals reconstituted with CD8<sup>+</sup> and CD4<sup>+</sup> T cells that were preincubated with anti-NKG2D and control antibody before cell transfer. Bederson score and grip test were evaluated 24h after 60-minutes tMCAO (CD8<sup>+</sup>: Rag1<sup>-/-</sup> n=10 vs. ctr. n=11 vs. αNKG2D n=6; CD4<sup>+</sup>: Rag1<sup>-/-</sup> n=8 vs. n=12 vs. αNKG2D n=12). (B) Global neurological deficits (Bederson score) and motor function (grip test) of CD1d<sup>-/-</sup> mice and γδ<sup>-/-</sup> animals 24h after 60-minutes tMCAO with and without pharmacological blockade of NKG2D (CD1d<sup>-/-</sup>: ctr. n=9 vs. αNKG2D n=12; γδ<sup>-/-</sup>: ctr. n=11 vs. αNKG2D n=12). (C) Functional scores of Rag1<sup>-/-</sup> mice supplemented with CD8<sup>+</sup> T cells from OT-1 mice as well as CD4<sup>+</sup> T cells from OT-2 mice 24h after tMCAO. T cells were pretreated *in vitro* with an anti-NKG2D blocking antibody and the respective isotype control (OT-1: ctr. n=8 vs. αNKG2D n=8; OT-2: ctr. n=9 vs. αNKG2D n=8). tMCAO: transient middle cerebral artery occlusion